MPK3/MPK6-mediated ERF72 Phosphorylation Positively Regulates Resistance to *Botrytis cinerea* Through Directly and Indirectly Activating the Transcription of Camalexin-biosynthesis Enzymes

Yihao Li[1], Kun Liu[1], Ganlu Tong[2], Chao Xi[1], Jin Liu[1], Heping Zhao[1], Yingdian Wang[1], Dongtao Ren[2] and Shengcheng Han[1,*]

1 Beijing Key Laboratory of Gene Resource and Molecular Development, College of Life Sciences, Beijing Normal University, Beijing 100875, China

2 State Key Laboratory of Plant Physiology and Biochemistry, College of Biological Sciences, China Agricultural University, Beijing 100094, China

E-mail address for Yihao Li, 290878447@qq.com; Kun Liu, 290744423@qq.com; Ganlu Tong, 591ziyou@163.com; Jin Liu, liujin@bnu.edu.cn; Chao Xi, xichao@bnu.edu.cn; Heping Zhao, hpzhao@bnu.edu.cn; Yingdian Wang, ydwang@bnu.edu.cn; Dongtao Ren, ren@cau.edu.cn.

* Corresponding Shengcheng Han, schan@bnu.edu.cn, ORCID ID: https://orcid.org/0000-0002-4039-7589.

To whom correspondence should be addressed:

Dr Shengcheng Han

Beijing Key Laboratory of Gene Resource and Molecular Development

College of Life Sciences

Beijing Normal University

Beijing 100875, China

E-mail: schan@bnu.edu.cn

Fax: +86-10-58807720

Abbreviations: ERF72, Ethylene response factor 72; MPK3/MPK6, Mitogen-activated protein kinases 3 and 6

Highlight

ERF72 coordinates the camalexin biosynthesis via directly activate *PAD3* and *CYP71A13* transcription or indirectly target *WRKK33*, and MPK3/6 phosphorylates ERF72 at Ser151 to improve its transactivation activity, camalexin contents and pathogen resistance.

Abstract

Ethylene response factor (ERF) Group VII members generally function in regulating plant growth and development, abiotic stress response, and plant immunity in *Arabidopsis*. However, the detail regulatory mechanism by which Group VII ERFs mediate plant immune responses remains elusive. Here, we characterised ERF72, a member of the Group VII ERFs, as a positive regulator mediating resistance to the necrotrophic pathogen *Botrytis cinerea*. Compared with wild type (WT), *erf72* mutant showed the lower camalexin contents and more susceptible to *B*. *cinerea*, while complementation of *ERF72* in *erf72* rescued susceptibility phenotypes. Moreover, overexpression of *ERF72* in WT promoted camalexin biosynthesis and resistance to *B*. *cinerea*. Then, we identified camalexin biosynthesis genes *PAD3* and *CYP71A13,* and transcription factor *WRKY33* as target genes of ERF72. Furthermore, MPK3 and MPK6 phosphorylate ERF72 at Ser151 to improve its transactivation activity, camalexin contents and resistance to *B*. *cinerea*. These findings highlight the role of ERF72 in coordinating the camalexin biosynthesis via directly regulating the expression of camalexin biosynthetic genes and indirectly by targeting WRKK33 in plant immunity.

Keywords: ERF72; MPK3/MPK6; WRKY33; PAD3; CYP71A13; camalexin biosynthesis; phosphorylation; pathogen resistance; *B cinerea*; *Arabidopsis.*

Introduction

Plants constantly confront a broad spectrum of pathogens throughout their lifecycles. According to their modes of obtaining nutrition from plant cells, pathogens fall into two types: biotrophs, which maintain a stable relationship with and feed on living host tissue (Glazebrook, 2005; Pieterse *et al.*, 2009); and necrotrophs, which destroy plant cells, often by secreting phytotoxins and cell wall-degrading enzymes, and derive nutrients from dead cells (Mengiste, 2012; Oliver and Ipcho, 2004). However, many phytopathogens display both lifestyles and are called hemibiotrophs (Oliver and Ipcho, 2004; Pieterse *et al.*, 2009). *Botrytis cinerea (B. cinerea)* is a necrotrophic fungal pathogen that has more than 200 plant species hosts and seriously impacts agricultural production (Dean *et al.*, 2012).

During coevolution with pathogens, plants have evolved physical barriers (Bigeard *et al.*, 2015) and produced antimicrobial secondary metabolites called phytoalexins for resistance to pathogens. In *Arabidopsis*, tryptophan-derived metabolites, including indole glucosinolates (IGS) and camalexin contribute to response to necrotrophic fungal pathogen (Bednarek, 2012; Piasecka *et al.*, 2015). In the process of camalexin biosynthesise, two homologous of cytochrome P450 enzymes CYP79B2 and CYP79B3 catalyse tryptophan to convert to indole-3-acetaldoxime (IAOx), then to indole-3-acetonitrile (IAN) by the P450 enzyme CYP71A13 (Nafisi *et al.*, 2007; Zhao *et al.*, 2002). By a series reaction to generate Cys(IAN), camalexin is later synthesized from Cys(IAN) by PAD3 (CYP71B15) (Bottcher *et al.*, 2009; Geu-Flores *et al.*, 2011; Schuhegger *et al.*, 2006; Su *et al.*, 2011; Wang *et al.*, 2012). Previous studies showed that destruction of camalexin biosynthesis pathway has enhanced susceptibility to necrotrophic pathogens like *B. cinerea* and *A. brassicicola* in *Arabidopsis* (Nafisi *et al.*, 2007; Wang *et al.*, 2012).

Plant recognition of pathogens triggers a series events, such as organelle [Ca^{2+}] increases, calcium-dependent protein kinases (CPKs) activation, mitogen-activated protein kinases (MAPKs) cascade activation, phytohormone production, and transcriptional reprogramming (Li *et al.*, 2016; Pieterse *et al.*, 2009). A prior study showed that activation of MPK3/MPK6, two pathogen-responsive MAPKs, is the mark event of early defence responses (Asai *et al.*, 2002). MPK3/MPK6 have been identified to participate in phytoalexins biosynthetic regulation (Ren *et al.*, 2008). Conditional induction of MPK3/MPK6 activity accumulates camalexin and indole glucosinolate, while *mpk3mpk6* double

mutant and MPK6SR, a chemical induced loss-of-function *mpk3mpk6* double mutant, show significantly reduce camalexin and IGS biosynthesis (Ren *et al.*, 2008; Xu *et al.*, 2016; Yang *et al.*, 2020). Moreover, some substrates of MPK3/MPK6 involved in phytoalexins biosynthesis have been identified. WRKY33, a key transcription factor regulating defence to necrotrophic pathogens, is phosphorylated by MPK3/MPK6 to enhance its transactivation activity, binds the W-box cis-element *TTGACC* in the promoters of camalexin biosynthetic genes *PAD3* and *CYP71A13* and positively regulates their expression (Mao *et al.*, 2011; Zhou *et al.*, 2020). In addition, WRKY57 is a negative regulator against *B. cinerea* infection and competes with WRKY33 to regulate the plant defence response (Jiang and Yu, 2016).

Ethylene response factor (ERF) is a large transcription factor family comprising 122 members classified into 12 groups in *Arabidopsis* (Huang *et al.*, 2016; Nakano *et al.*, 2006). ERFs usually bind to the GCC-box cis-element GCCGCC, which is frequently present in the promoter regions of pathogen-induced genes (Catinot *et al.*, 2015; Meng *et al.*, 2013; Pre *et al.*, 2008). Meng *et al* (2013) showed that ERF6 activates defence-related genes *PDF1.1* and *PDF1.2* in an ethylene-independent pathway in response to *B. cinerea* infection in *Arabidopsis*. Moreover, ERF6 directly regulates the expression of *CYP81F2* and *IGMT1/IGMT2*, which encode key enzymes in the biosynthesis of the antimicrobial compound indole glucosinolates (Xu *et al.*, 2016). In addition, *ERF5* has been shown to be a redundancy gene of *ERF6*, because *erf5 erf6* double mutants show significant susceptibility to *B. cinerea*, but single mutants do not (Moffat *et al.*, 2012). In *Arabidopsis*, pathogens trigger MPK3 and MPK6 activation within a few minutes, and ERF6 also can be phosphorylated by MPK3 and MPK6 in response to *B. cinerea* infection to increase its protein stability (Mao *et al.*, 2011; Meng *et al.*, 2013).

ERF Group VII (ERF-VII) has five members which share the conserved N-terminal sequence MCGGAI/L to be recognized for degradation through the Cys-Arg/ N-degron pathway, and play a vital role in low oxygen and nitric oxide (NO) sensing (Gibbs *et al.*, 2011; Gibbs *et al.*, 2014; Licausi *et al.*, 2011; Licausi *et al.*, 2013b). In normal oxygen and nitric oxide conditions, N-terminal cysteine residue of ERF-VII proteins are exposed and oxidized by the plant cysteine oxidases (PCOs), then targeted for proteasomal degradation via Cys-Arg/ N-degron pathway. Under hypoxia condition, oxidation of cysteine is blocked, or cysteine is artificially mutated to stabilizing residues, such as alanine, ERF-VII proteins disable the recognition and degradation by the Cys-Arg/ N-degron pathway, which improves its stabilization (Weits *et al.*, 2014; White *et al.*, 2018). Current researches demonstrated that the

stabilization of ERF-VII regulated by Cys-Arg/ N-degron pathway plays important roles in defence against pathogens. RAP2.2, a member of ERF-VII, is involved in defence response to *B. cinerea*. Overexpression of *RAP2.2* enhanced resistance to *B. cinerea*, whereas *rap2.2* mutant showed more sensitive (Zhao *et al.*, 2012). ERF72 (related AP2 3, RAP2.3) also seems to mediate defence possibly via interacting with the acyl-CoA binding protein ACBP4 (Li *et al.*, 2008). *erf72* mutant showed more resistant to *Fusarium oxysporum,* a root-infecting fungal pathogen (Chen *et al.*, 2014). Moreover, *B. cinerea* infection induces the local hypoxia, which increases the stabilization of ERF-VII proteins and promotes their translocation to the nucleus (Valeri *et al.*, 2021). However, the detail mechanism of ERF-VII members involved in plant defence response remain elusive.

In this study, we characterised the role of ERF72 in regulating resistance against *B. cinerea*. Compared with WT, *erf72* was more susceptible to *B. cinerea*, while overexpression of *ERF72* promoted resistance. Furthermore, ERF72 regulates camalexin biosynthesis through directly targeting *PAD3* and *CYP71A13* and indirectly targeting *WRKY33* transcription. In addition, MPK3/MPK6 phosphorylate ERF72 at Ser151 to improve its transcriptional activation. These findings reveal a novel mechanism on ERF72 phosphorylation by MPK3/MPK6 regulating plant immunity in plants.

Materials and Methods

Plant Materials and Growth Conditions

Arabidopsis thaliana plants (Col-0 ecotype) were used in this study. The mutants *erf72* (CS849696), *wrky33* (Salk_006603) and *erfVII*, and transgenic lines ERF72ox (*p35S: ERF72-HA* in WT), $MKK5^{DD}$(steroid-inducible promoter:$MKK5^{DD}$), MPK6SR (*pMPK6:*$MPK6^{YG}$ in *mpk3 mpk6*) have been described previously (Supplemental Table S1) (Gibbs *et al.*, 2014; Liu *et al.*, 2008; Liu *et al.*, 2018; Xu *et al.*, 2014; Zheng *et al.*, 2006). The transgenic plants Com-MC [*pERF72:(MC)ERF72-HA* in *erf72*], Com-MA [*pERF72:(MA)ERF72-HA* in *erf72]* and ERF72ox/MPK6SR (*p35S:ERF72-3HA* in *MPK6SR*), were generated in this study. All DNA fragments were amplified with the listed primers (Supplementary Table S2) and plasmids were constructed as previously described (Supplemental Table S3) (Liu *et al.*, 2018). The constructs were introduced into *Agrobacterium* GV3101 by electroporation, then transformed into *Arabidopsis* by the floral dip method (Clough and Bent, 1998). Single-insertion lines were collected and protein levels were detected by immunoblot. F3 homozygous transgenic plants were used in this study. ERF72ox/*wrky33* and $MKK5^{DD}$ in *erf72* were generated by crossing and F2 homozygous plants were used for the experiments (Supplementary Table S1).

Seeds were sterilised with 75% ethanol and sown on half-strength Murashige & Skoog (1/2MS) medium with 1.5% sucrose and 0.8% agar. The seeds were incubated at 4 °C under dark conditions for 2 d, then transferred to a growth chamber at 22 °C under a 16-h light (100 μmol m^{-2} s^{-1}) / 8-h dark cycle. Seven-day-old seedlings were planted in soil, and then grown under the same growth conditions in a greenhouse for pathogen infection and protoplast isolation.

Protein Extraction and Immunoblot Analysis

14-day-old liquid cultured seedlings were collected at various time points following inoculation with *B. cinerea* spores (5×10^5 spores/mL) or mock treatment, then ground in liquid nitrogen. Total proteins were extracted with extraction buffer containing 50 mM Tris-HCl (pH 6.8), 2% sodium dodecyl sulphate (SDS), 10% glycerine, 1 mM β-mercaptoethanol, and 1X protease inhibitor cocktail (Roche, Basel, Switzerland). Protein samples were separated by 12% SDS-polyacrylamide gel electrophoresis (PAGE) and transferred to a PVDF membrane (Millipore, Burlington, MA, USA). Immunoblots were performed using antibodies were used at the following dilutions: anti-HA antibody (1:5000 dilution; Sigma-Aldrich, St. Louis, MO, USA), anti-pERK (1:2000 dilution, Cell Signalling, Danvers, MA, USA),

HRP-linked anti-mouse IgG and HRP-linked anti-rabbit IgG (1:2000 dilution, Cell Signalling, Danvers, MA, USA). Signals were detected on a 5200 Luminescent Imaging Workstation (Tanon, Shanghai, China) using Immobilon Western Chemiluminescent HRP (Millipore, Burlington, MA, USA).

Pathogen Infection Assay

B. cinerea was cultivated on 2× V8 agar medium (36% V8 juice, 0.2% $CaCO_3$, and 2% agar) for 10 days at 22 °C. Spores were collected, washed, and adjusted to a concentration of 5×10^5 spores/mL in Vogel-Johnson medium. For drop inoculation of *Arabidopsis* leaves, 5 µL of spore suspension was dropped onto 4-week-old detached leaves and incubated under high humidity at 22°C. Leaf phenotypes were photographed at 2 or 3days after inoculation and lesion diameters were measured using ImageJ software.

qRT-PCR Analysis

Total RNA was extracted from seedlings of 14-day-old liquid cultured plants treated with *B. cinerea* spores using a Total RNA Extraction Kit (Promega, Madison, WI, USA). 1.5 µg total RNA was reverse transcribed to first-strand cDNA using cDNA Synthesis SuperMix (Transgen Biotech, Beijing, China). qPCR was performed using Eastep qPCR Master Mix (Promega) with the QuantStudio 6 Flex Real-Time PCR System (Thermo Fisher, Waltham, MA, USA). Relative expression of target genes was normalized to *RGS1-HXK1 Interacting Protein 1* (*AtRHIP1*, AT4G26410) that was described as highly constant under varying stress conditions (Czechowski *et al.*, 2005) and *AtActin2* (Maruyama *et al.*, 2013). At least three biological replicates were performed for each experiment.

Electrophoretic Mobility Shift Assay (EMSA)

EMSA was performed as described previously (Zong *et al.*, 2016). The His-ERF72-HA recombinant protein was expressed in *Escherichia coli* at 25 °C for 16 h with the induction of 0.2 mM Isopropyl-beta-D-thiogalactopyranoside (IPTG) and purified using His Sepharose beads (General Electric Company, Boston, MA, USA). 5-FAM-labeled and unlabelled oligonucleotides were synthesised by Ruibiotech Company (Beijing, China). His-ERF72-HA was incubated with annealed double-stranded oligos in binding buffer (Beyotime Biotechnology, Jiangsu, China) at room temperature for 30 min. The samples were separated by 8% native-PAGE with 0.5× TBE buffer at 4°C in the dark for 1.5 h. Fluorescence was captured using a 5200 Luminescent Imaging Workstation.

ChIP-qPCR assay

Arabidopsis Com-MA lines were used for ChIP-qPCR assays as described previously (Liu *et al.*,

2018). 14-day-old liquid-cultured seedlings were collected and ground in liquid nitrogen, then cross-linked with 1% formaldehyde and terminated with glycine. The nuclear pellet was extracted, lysed, and sonicated in a Bioruptor (UCD-200, Diagenode, Denville, NJ, USA) to yield DNA fragments of ~500 bp. Immunoprecipitation was performed using Dynabeads Protein G (Life Technologies, Carlsbad, CA, USA) and bound with anti-HA antibody or anti-mouse IgG (Abcam, Cambridge, UK) overnight at 4 °C, and the immunoprecipitated DNA was purified for qPCR analysis with the specific primers listed in Supplementary Table S2.

Bimolecular Fluorescence Complementation (BiFC) Assays

The coding regions of *MPK3* and *MPK6* were cloned into the *pSPYNE173* vector to generate MPK3-nYFP and MPK6-nYFP, and the coding region of *ERF72* was cloned into *pSPYCE(M)* to obtain ERF72-cYFP (Waadt *et al.*, 2008). Each construct was transformed into *Agrobacterium tumefaciens* GV3101 by electroporation. All *Agrobacterium* strains were cultured overnight, and resuspended and adjusted in infiltration buffer (10 mM MES, 10 mM $MgCl_2$, and 100 μM acetosyringone) to OD_{600} = 1.0. After incubation at room temperature for 2 h, an equal volume of the agrobacterial suspension harbouring the two different constructs was mixed with the *p19* strain and infiltrated into 4-week-old leaves of *Nicotiana benthamiana*. The yellow fluorescence protein (YFP) fluorescence signal was imaged by a confocal microscope (LSM700, Zeiss, Oberkochen, Germany) after a 3-d infection.

Pull-down Assay

The pull-down assay was performed as previously described (Xu, 2020). Briefly, recombinant GST-MPK3 and GST-MPK6 proteins were purified using glutathione beads (Sangon, Shanghai, China), then incubated with 5 μg His-ERF72-HA at 4 °C for 2 h in NETN buffer (20 mM Tris-HCl, 100 mM NaCl, 0.5 mM EDTA, 0.5% (v/v) IGEPAL CA-630, pH8.0). After removing the supernatant, the beads were washed by NETN buffer five times. Protein samples were eluted by boiling the beads in SDS sample loading buffer, separated by SDS-PAGE and analyzed by Immunoblot as described.

In Vitro Phosphorylation Assay

The in vitro phosphorylation assay was performed as described previously with minor modification (Mao *et al.*, 2011). Recombinant His-tagged MPK3 or MPK6 were incubation with $MKK5^{DD}$ in the kinase reaction buffer (25 mM Tris-HCl, pH7.5, 10mM $MgCl_2$, 1mM DTT, 50 μM ATP) at 25℃ for 0.5 h. His- and HA-tagged bacterially expressed ERF72 protein and $ERF72^{S151A}$ mutant protein were incubated with the activated MPK3 or MPK6 in the kinase reaction buffer at 25 °C for 0.5 h. The

samples were separated by 6% SDS-PAGE gel containing 75 mM Phos-tag (Wako, Japan) and 200 mM $MnCl_2$ and detected by immunoblot as described.

Cell-free Semi-in Vivo Phosphorylation Assay

14-day-old liquid-cultured seedlings were harvested at indicated time points following treatment with *B. cinerea* spores (5×10^5 spores / mL) or 2 μM DEX. The samples were ground in liquid nitrogen and resuspended in extraction buffer (20 mM HEPES pH7.5, 10 mM $MgCl_2$, 1mM DTT, 1X protease inhibitor cocktail and 25 μM MG132) on ice. Supernatant was separated by centrifuging at 12,000 g at 4 °C for 10 min. A final concentration of 10 μM ATP and 2 μg His- and HA-tagged bacterially expressed ERF72 protein were added to the cell lysates and kept at 25 °C for 1 h. The reactions were stopped by adding SDS sample loading buffer and boiling for 5 min. The samples were separated by 12% SDS-PAGE gel or 6% Phos-tag gel, then detected by immunoblot as described.

Transient Gene Expression Assays

The promoter region of *PAD3* and *CYP71A13* were amplified by PCR from *Arabidopsis* genomic DNA and inserted into the SalI and KpnI restriction sites of the plasmid *pCambia1305.1* to generate *pPAD3:GUS* and *pCYP71A13:GUS* constructs. *pWRKY33: GUS* was cloned into *pCambia1305.1* by BamHI and HindIII with the same method. The transient gene expression assays were performed as described previously (Liu *et al.*, 2018). *Arabidopsis* mesophyll protoplasts (2×10^5) were isolated from 4-week-old rosette leaves, transfected with 30 μg of DNA (effector : reporter : internal standard = 5:4:1), harvested after 12 h, and lysed in 100 μL of passive lysis buffer (Promega, USA). The GUS activity was measured using methyl umbelliferyl glucuronide (working concentration at 1 mM) and detected the fluorescence values with 365-nm excitation and 445-nm emission by FlexStation 3 Microplate Reader (Molecular Devices, USA). Firefly luciferase activity were assayed using Steady Glo Luciferase Assay System (Promega, USA). The ratio of GUS / luciferase activity was used to determine the promoter activity.

Camalexin Content Measurement

Camalexin contents were measured as previously described (Yang *et al.*, 2020). 7-day-old seedlings grown on 1/2MS medium were transferred to 7 mL of liquid culture medium in 40-mL gas chromatography vials, and cultured under continuous light for 10 d. Then, the seedings were treated with *Botrytis cinerea* spores (5×10^5 spores per vial), 1 μM Dex, 2 μM NA-PP1 or equal volume solvent as control. The liquid medium was harvested at the indicated time points after different

treatment. Fluorescence values were measured by F-4500 Fluorescence Spectrophotometer (Hitachi, Japan) with wavelength of excitation at 315 nm and emission at 385 nm. The standard curve was established by using camalexin standard samples.

Statistical Analysis

Statistical analyses were performed using GraphPad Prism 7.0 software. Student's *t*-test was conducted to evaluate the statistical significance between two group of data at a single time point. One-way analysis of variance (ANOVA) with Tukey's post-hoc test was performed to determine the significance of differences among different genotypes at a single time point. Two-way ANOVA followed by Tukey's post-hoc test was used to the statistical significance between different group at different time point. The statistically significant difference was denoted by different letters or asterisks.

Results

ERF72 is a Positive Regulator for Camalexin Production Upon B. cinerea Infection

To evaluate the role of ERF72 in resistance to *B*. *cinerea*, we first observed the *B*. *cinerea* infection phenotypes of 4-week-old detached *Arabidopsis* leaves from WT and *erf72*. At 2 d post drop inoculation, *erf72* showed larger lesions than WT (Fig. 1A and 1B). To further confirm the *B. cinerea* sensitive phenotype caused by ERF72 mutant, we generated two transgenic lines that complemented the expression of wild type form of *ERF72* (*MC-ERF72*) driven by a 2553-bp native promoter (Com-MC #3 and #9). RNA level of the transgenic lines was similar to WT and protein levels of ERF72 could be detected after proteasome inhibitor MG132 treatment (Supplementary Fig. S1). To evaluate the *B*. *cinerea* infection phenotype, we inoculated *B*. *cinerea* spores on detached leaves and found that both transgenic lines could rescue the susceptibility phenotypes of *erf72* (Fig. 1A and 1B). Furthermore, we generate the transgenic lines that expressed a stable form of *ERF72* (*MA-ERF72*) driven by a native promoter in *erf72* (Com-MA #2 and #8), in which the second Cys was mutated to a stabilizing residue Ala, preventing ERF72 degradation by the Cys-Arg/ N-degron pathway (Gibbs *et al.*, 2011), and the transgenic lines that overexpressed *MC-ERF72* driven by the CaMV 35S promoter in WT plants (ERF72ox #107 and #108). RNA levels of Com-MA and ERF72ox lines were greatly higher than that of WT, and protein levels of Com-MA and ERF72ox lines was detectable without MG132 treatment, and accumulated after MG132 treatment (Supplementary Fig. S1). Then, we found that both the leaves of Com-MA and ERF72ox lines presented smaller disease spots than that of WT (Fig. 1A and 1B, Supplementary Fig. S2A and S2B), suggesting that promoting the transcript and protein levels of ERF72 enhances the resistant to *B. cinerea*. To further characterize the fungal growth in planta, 4-week-old plant were sprayed with *B. cinerea* spores for 2 or 4 d and the expression level of fungal *Actin A* (*BcActin A*) was monitored by qRT-PCR according to a prior study (Zhao *et al.*, 2012). Similar with the result of drop inoculation, the biomass of *B. cinerea* was more abundant in *erf72* than WT, whereas Com-MC and Com-MA lines have the same level of *B. cinerea* biomass as WT, and less *B. cinerea* accumulated in ERF72ox lines at 4 d after inoculation than that in WT (Supplementary Fig. S3). We also detected the expression of defensive marker gene *PDF1.2* in WT and *erf72* plants sprayed with *B. cinerea* spores at 2 and 4 d, and found that the expression of *PDF1.2* was promoted in both WT and *erf72* after sprayed with *B. cinerea* spores, and the expression level of *PDF1.2* is

higher in *erf72* than that in WT at 2 and 4 d with the treatment of *B. cinerea* (Supplementary Fig. S4). These results indicated that *B. cinerea* sensitive phenotype presented in *erf72* is not related to the expression of *PDF1.2*.

Previous studies showed that camalexin is produced upon pathogen challenge and functions in defense responses (Glawischnig, 2007; Møldrup *et al.*, 2013), so we measured camalexin contents in 17-day-old liquid cultured seedling of WT, *erf72*, different complemented and overexpressed lines after challenged with *B. cinerea*. We found that, compared with that in WT, camalexin production were lower in *erf72* at 24 h post inoculation, while Com-MC and Com-MA plants have rescued camalexin content in *erf72* (Fig. 1C and Supplementary Fig. S2C). In addition, overexpressing lines have the similar camalexin content at 12 h and 24 h after *B. cinerea* inoculation as WT (Fig. 1C). We further monitored *B*. *cinerea* infection phenotypes in 4-week-old detached leaves and camalexin contents in liquid cultured seedlings from *erfVII* pentuple mutant and found that, compared with WT, *erfVII* showed larger lesions in leaves, but no difference of camalexin contents in liquid cultured seedlings (Supplementary Fig. S5).

A recent study showed that *B. cinerea* infection induces local hypoxia and allows the stabilization of ERF-VII proteins (Valeri *et al.*, 2021). To monitor the change of ERF72 protein level in Com-MC, Com-MA and ERF72ox lines during *B. cinerea* inoculation, we inoculated the seedlings with *B. cinerea* spores at different time points, and found that ERF72 was accumulated at 6 h and reached a peak at 12 h, then decreased at 24 h during *B. cinerea* infection period in both Com-MC and ERF72ox lines (Fig. 1D), but the protein level is stable in Com-MA lines (Supplementary Fig. S2D). Similar to the results showed in Valeri *et al* (2021), we also found that the expression of *ALCOHOL DEHYDROGENASE 1* (*ADH1*), *PCO1*, and *PYRUVATE DECARBOXYLASE 1* (*PDC1*) are induced with *B. cinerea* inoculation in both WT and *erf72* plants (Supplementary Fig. S6). However, the expression level of these three genes was markedly lower at 12-h inoculation of *B. cinerea* in *erf72* than that in WT (Supplementary Fig. S6), suggesting that the expression of these genes is regulated by ERF72. These results indicated that *B. cinerea* infection improves the protein stability of ERF72, and ERF72 acts as a positive regulator for camalexin formation against *B. cinerea* infection in *Arabidopsis*.

ERF72 Directly Targets Genes of Camalexin Biosynthesis

It was well proved that PAD3 and CYP71A13 are two key enzymes for camalexin biosynthesis in *Arabidopsis* (Bottcher *et al.*, 2009; Nafisi *et al.*, 2007; Schuhegger *et al.*, 2006). Therefore, we firstly investigated the expression levels of *PAD3* and *CYP71A13* in WT and *erf72* after *B. cinerea* inoculation, and found that the expression of *PAD3* and *CYP71A13* are upregulated with *B. cinerea* inoculation in both WT and *erf72* plants (Fig. 2A and Supplementary Fig. S7). However, the expression level of *PAD3* was markedly lower at 12-h and 24-h inoculation of *B. cinerea* in *erf72* than that in WT, and that of *CYP71A13* was just slightly lower at 12-h and 24-h inoculation of *B. cinerea* in *erf72* compared with WT (Fig. 2A). These results indicated that the expression of *PAD3* and *CYP71A13* is strictly regulated by ERF72 besides another main transcription factor WRKY33 in *Arabidopsis* (Birkenbihl *et al.*, 2012; Qiu *et al.*, 2008).

Generally, ERF binds to the GCC box (AGCCGCC) in the promoter of target genes to activate or inhibit its expression (Allen *et al.*, 1998; Fujimoto *et al.*, 2000; Hao *et al.*, 1998). Although there was no canonical GCC box found in the promoter region of *PAD3* and *CYP71A13*, one GCC-like box, AGCCGTC at −652 bp from the translation start site at complementary strand or AGCCGAC at -329 bp from the translation start site at complementary strand was predicted in each promoter, respectively (Supplementary Fig. S8). We performed the transient transactivation assays in *Arabidopsis* protoplasts to test whether ERF72 directly activate the transcriptional activity of promoters of *PAD3* and *CYP71A13*, and showed that (MA)ERF72 can effectively activate the promoter activities of both genes which were fused to *GUS* gene as reporter constructs *pPAD3:GUS* and *pCYP71A13:GUS* (Supplementary Fig. S8 and Fig. 2B). Moreover, using *(MA)ERF72-HA*-overexpressed *Arabidopsis* seedlings, ChIP-PCR was carryout to examine the binding of ERF72 in the promoter of *PAD3 and CYP71A13* in vivo. As shown in Fig. 2C, anti-HA antibody efficiently enriched the DNA fragment containing GCC-like box of *PAD3* and *CYP71A13* promoter, respectively. In addition, EMSA showed that ERF72 can bind to the FAM-labelled GCC-like box probes of *PAD3* or *CYP71A13* promoter to produce a shift band of probe (Fig. 2D). And, unlabelled cold probe effectively competed the bind with ERF72 to attenuate the shift band, while the mutant form of GCC-like box had no competition effect with labelled probe for binding with ERF72 (Fig. 2D). There results proved that both *PAD3* and *CYP71A13* are the target genes of ERF72.

WRKY33 is Also a Target Gene of ERF72

WRKY33 was well characterized as a positive regulator for camalexin biosynthesis in the response to *B. cinerea* infection in *Arabidopsis* (Birkenbihl *et al.*, 2012; Zheng *et al.*, 2006). Therefore, we monitored the transcription level of *WRKY33* in *erf72* after challenged with *B. cinerea.* Compared to WT, *WRKY33* expression was markedly suppressed in *erf72* post *B. cinerea* incubation (Fig. 3A and Supplementary Fig. S7). Moreover, a typical GCC box was predicted to be located at −123 bp upstream of the translation start site of *WRKY33* (Supplementary Fig. S8). Therefore, we firstly performed a transient transactivation assay using the *WRKY33* promoter (*pWRKY33*, −1496 to −1) and its mutated GCC box form fused to the GUS gene as a reporter and *p35S:(MA)ERF72* as an effector, separately, and found that ERF72 activates transcriptional activity of *pWRKY33*, but not its mutated GCC box form (Fig. 3B). Moreover, EMSA showed that ERF72 specifically binds to the GCC box of *pWRKY33* (Fig. 3C). In addition, ChIP-qPCR showed that the GCC box of *pWRKY33* was enriched by ERF72 *in vivo* (Fig. 3D). These results indicated that ERF72 upregulates *WRKY33* transcription via directly binding to the GCC box in *pWRKY33* in *Arabidopsis*.

ERF72 Bypasses WRKY33 to Regulate Camalexin Biosynthesis and Resistance to B. cinerea.

To distinguish the role of ERF72 and WRKY33 on camalexin biosynthesis in response to *B. cinerea* infection, we generated *ERF72-overexpressed* in *wrky33* plants (*ERF72ox/wrky33* #7 and #8) (Supplemental Fig. S9). When drop-inoculated with *B. cinerea*, lesion sizes of ERF72ox/*wrky33* #7 and #8 were similar to *wrky33*, and larger than that of WT (Fig. 4A and 4B). Furthermore, we found that camalexin contents in ERF72ox/*wrky33* plants are higher than that in *wrky33*, but lower than that in WT at 12 or 24 h post inoculation with *B. cinerea* (Fig. 4C). In addition, overexpression of *ERF72* in *wrky33* didn't entirely rescue the expression defects of *PAD3* and *CYP71A13* in *wrky33* (Fig. 4D and Supplementary Fig. S10). These data suggested that ERF72 positively regulates the transcription of *PAD3* and *CYP71A13* partially independent on WRKY33. To further investigate the genetic interaction between *ERF72* and *WRKY33*, we generated *erf72 wrky33* double mutant (Supplementary Fig. S11). Compared with *erf72*, the *erf72 wrky33* displayed enhanced susceptibility to *B. cinerea* and decreased camalexin content induced by *B. cinerea*, that is similar to *wrky33* (Fig. 4E-G). These results further support that ERF72 acts the upstream of WRKY33.

MPK3/MPK6 phosphorylate ERF72 at Ser151 in response to B. cinerea infection

An *in vitro* kinase assay showed that ERF72 at Ser151 is phosphorylated by activated MPK3 and MPK6 extracted from flg22-induced *Arabidopsis* cell cultures (Sorensson *et al.*, 2012). However, the

phosphorylation of ERF72 by MPK3/MPK6 upon *B. cinerea* challenge remains unclear. Therefore, we first monitored the interaction of ERF72 with MPK3 or MPK6 *in vivo* by BiFC experiments. Co-expression of MPK3- or MPK6-nYFP with ERF72-cYFP in tobacco leaves led to reconstitution of the YFP signal in the nucleus, but no YFP signals were observed in empty vector controls (Fig. 5A). The interaction was further verified by an in vitro pull-down assay. The His-ERF72-HA protein was pulled down by GST-MPK3 and GST-MPK6 protein, but not the GST protein alone (Fig. 5B). These results indicate that ERF72 directly binds to MPK3 and MPK6 in vitro and in vivo.

To verify ERF72 as a substrate of MPK3 and MPK6, we performed in vitro phosphorylation following with Phos-tag mobility shift assays. Shifted bands were observed when ERF72 was incubated with activated MPK3 and MPK6. These upshift bands were abolished after mutating Ser151 residue to Ala ($ERF72^{S151A}$), indicating that Ser151 of ERF72 is phosphorylated by MPK3/MPK6 in vitro (Fig. 5C). Because of ERF72 hardly detected in planta, we prepared a His- and HA-tagged recombinant ERF72 protein for semi-in *vivo* MAPK phosphorylation assays detected by Phos-tag gel. A Prior study showed that dexamethasone (DEX)-induced constitutively active form of MKK5 ($MKK5^{DD}$) plant was generated, which activates MPK3/MPK6 by DEX treatment (Ren *et al.*, 2008). His-ERF72-HA was incubated with protein extracts from $MKK5^{DD}$ plants per-treated with or without DEX. Then, a shift band was observed in a Phos-tag SDS-PAGE gel when His-ERF72-HA was incubated with extracts from DEX-treated $MKK5^{DD}$ plants, but absent in $ERF72^{S151A}$ (Fig. 5D). To further demonstrate the phosphorylation of ERF72 by MPK3/MPK6 during *B. cinerea* infection, recombinant ERF72 or $ERF72^{S151A}$ protein was incubated with protein extracts from WT seedling pre-treated with *B. cinerea* or not. We found a shift band appeared when ERF72 inoculated with protein extracts from *B. cinerea* infested plants. By contrast, no such shift appeared when $ERF72^{S151A}$ inoculated with protein extracts from *B. cinerea* infested plants (Fig. 5E). These results proved that MPK3/MPK6 phosphorylates ERF72 at Ser151 upon *B. cinerea* infection in plants.

Phosphorylation of ERF72 by MPK3/MPK6 Enhances its Transactivation Activity

To explore the transactivation role of ERF72 phosphorylation by MPK3/MPK6, we separately constructed plant expression vectors containing $ERF72^{S151A}$, a non-phosphorylation form, or $ERF72^{S151D}$, a constitutive phospho-mimic form. Using a transient transactivation assay, we found that $ERF72^{S151D}$, similarly to *ERF72*, effectively activates *pWRKY33:GUS*, but $ERF72^{S151A}$ has no transactivation activity for *pWRKY33:GUS* (Fig. 6A). Moreover, co-transformation of *ERF72* and a

continuously activated form *MKK5*^{DD} can activate *pWRKY33:GUS* more effectively than single transformation of *MKK5*^{DD} and co-transformation of *ERF*^{S151A} with *MKK5*^{DD} in *Arabidopsis* mesophyll protoplasts (Fig. 6B). Furthermore, we generated the MKK5^{DD} *erf72* plant by crossing MKK5^{DD} with *erf72* to detect camalexin production and associated genes expression after DEX treatment. Firstly, we found that there was no obvious difference in MPK3/MPK6 activity between MKK5^{DD} and MKK5^{DD} *erf72* upon DEX treatment using anti-pERK antibody as detection probe (Fig. 6C). After DEX treatment, camalexin contents increased in MKK5^{DD} plant, but synthesis retardation was observed in the MKK5^{DD} *erf72* background (Fig. 6C). We also found that the transcriptions of *WRKY33*, *PAD3 and CYP71A13* in the MKK5^{DD} background are greatly induced, but was significantly impaired in the MKK5^{DD} *erf72* following treatment with DEX (Fig. 6D and Supplementary Fig. S12). Taken together, these results suggested that MPK3/MPK6 phosphorylation of ERF72 is critical for its transactivation activity and camalexin biosynthesis.

Phosphorylation of ERF72 by MPK3/MPK6 is Essential for Resistance to B. cinerea

In a prior study, Xu *et al* (2014) introduced *MPK6*^{YG}, a kinase inhibitor NA–PP1 (4–amino-1–tert-butyl-3–(1′–naphthyl)pyrazolo[3,4–d]pyrimidine)-sensitive MPK6 variant, driven by its native promoter into *mpk3 mpk6* double mutant to generate the *MPK6SR* line (genotype *mpk3 mpk6* $_{P}$*MPK6:MPK6YG*). In the absence of NA–PP1, MPK6^{YG} is functional and enable rescue of the embryo lethality of *mpk3 mpk6*; and in the presence of NA-PP1, MPK6 kinase activity can be temporally blocked. Therefore, we generated *ERF72-overexpresseded* in *MPK6SR* lines (*ERF72ox/MPK6SR*) #4 and #5 to characterise the function of ERF72 phosphorylation by MPK3/MPK6 on the defence response to *B. cinerea* (Supplementary Fig. S13). Without NA-PP1 treatment, *ERF72ox*/*MPK6SR* #4 and #5 exhibited similar pathogen infection phenotypes as WT and *MPK6SR* after 2 days of *B. cinerea* inoculation, but showed greater resistance to *B. cinerea* than WT and MPK6SR on the 3rd day of infection (Fig. 7A and 7B). However, pre-treatment with NA-PP1 for 12 h led to more susceptibility to *B. cinerea* for *ERF72ox*/*MPK6SR* #4 and #5 than that in WT, and less susceptibility to *B. cinerea* than that in MPK6SR after 2 days of infection (Fig. 7A and 7B). Subsequently, we detected the *B. cinerea*-induced camalexin accumulation in in WT, *MPK6SR*, and *ERF72ox/MPK6SR* plants. Without NA-PP1 treatment, there was no obvious difference of camalexin content among WT, *MPK6SR*, and *ERF72ox*/*MPK6SR* #4 and #5 lines (Fig. 7C). Following pre-treatment with NA-PP1, camalexin contents significantly reduce in *MPK6SR* and *ERF72ox/MPK6SR* plants, but not in WT (Fig. 7C).

These results suggested that MPK/MPK3-mediated ERF72 phosphorylation is required for camalexin biosynthesis in response to *B*. *cinerea* inoculation in *Arabidopsis*.

Discussion

Facing phytopathogen infection, plants accumulate phytoalexin for pathogen resistance. Camalexin is the major phytoalexin in *Arabidopsis*, its biosynthetic pathways and transcriptional regulators of related key enzymes have been well characterized (Piasecka *et al.*, 2015). Pathogen-responsive MPK3/MPK6 have been reported to play the critical role in *B. cinerea* induced camalexin production (Ren *et al.*, 2008). Previous studies showed that MPK3/MPK6 active the expression of camalexin biosynthesis genes, such as *PAD3* and *CYP71A13*, through phosphorylating and enhancing the transactivation activity of *WRKY33* (Mao *et al.*, 2011; Zhou *et al.*, 2020). In addition, WRKY33 activates the transcription of *WRKY33* to form a feedback loop for pathogen resistance (Mao *et al.*, 2011). In this study, we revealed a MPK3/MPK6 phosphorylation of ERF72-mediated accessory pathway in regulating camalexin biosynthesis and resistance to *B. cinerea* in *Arabidopsis*. We found that *erf72* exhibits low camalexin content and decreased resistance against *B. cinerea*, while constitutive expression of ERF72 in WT resulted in significantly increased camalexin production and pathogen resistance. Moreover, MPK3/MPK6-phosphorylated ERF72 regulated camalexin biosynthesis by two pathways: directly activating the transcription of *PAD3* and *CYP71A13,* and indirectly through transactivation of *WRKY33*. Therefore, our results provided a new MPK3/6-mediated transcriptional regulation mechanism on camalexin biosynthesis in response to necrotrophic pathogen challenge in plants.

ERFs integrate phytohormone signalling and the MAPK pathway to regulate the expression of defence genes (Huang *et al.*, 2016; Licausi *et al.*, 2013a). Recent studies showed that ERF Group VII members contribute to *Arabidopsis* resistance to necrotroph fungi (Kim *et al.*, 2018; Valeri *et al.*, 2021; Zhao *et al.*, 2012). However, few direct target genes of ERF VII transcription factor have been identified. Here, we demonstrated ERF72 binding to the promoter regions of *PAD3*, *CYP7A13* and *WRKY33* containing canonical GCC or GCC-like box and directly upregulating their expression. ORA59, another ERF, is also targeted by WRKY33 and regulate resistance to necrotrophic pathogens (Birkenbihl *et al.*, 2012; Pre *et al.*, 2008; Zander *et al.*, 2014). ORA59 interacts with ERF72 and both

translocated to the nucleus in ethylene-dependent manner (Kim *et al.*, 2018), suggesting that ERF72-WRKY33-ORA59 possibly formed a positive feedback loop to enhance defense-related genes expression. Our prior study showed that *ERF72* interacts with Auxin Response Factor 6 (ARF6), Brassinazole-resistant 1 (BZR1) and DELLA to integrate light and phytohormone signals, such as BR, auxin, ethylene and GA, and regulate photomorphogenesis-related hypocotyl elongation and apical hook development in *Arabidopsis* (Liu *et al.*, 2018). These results indicated that ERF72 act as a key transcriptional regulator to regulate plant growth, development, and adaption to various environmental stresses by directly regulating gene expression and/or interacting with other transcription factor.

Previous studies showed that the members of ERF-VII are known as the substrates of the Cys-Arg/N-degron protein degradation pathway and critical for oxygen and nitric oxide sensing in plants (Gibbs *et al.*, 2011; Gibbs *et al.*, 2014; Licausi *et al.*, 2011; Licausi *et al.*, 2013b). Recent reports have shown that the Cys-Arg/N-degron pathway contribute to pathogen resistance (de Marchi *et al.*, 2016; Vicente *et al.*, 2019). Cys-Arg/N-recognin specific E3 ligase mutants *prt6*, enhanced resistance to the hemi-biotrophic pathogen *Pseudomonas syringae* pv. tomato DC3000 through regulating the expression of *CYP71A12/A13, GSTF6*, and *PAD3* to increase camalexin contents (Vicente *et al.*, 2019). These results would be explained that stabilization of ERF72 improves the expression of *CYP71A13* and *PAD3*. However, the expression of *PDF1.2* was higher in *erf72* than WT, suggesting that the *B. cinerea* sensitive phenotype is not associated to the expression of *PDF1.2*, while other ERFs may enhance *PDF1.2* expression in *erf72* in response to *B. cinerea* inoculation. We also found that *B.cinerea* infection improves protein stabilization of ERF72 which activates the transcription of hypoxia marker genes, such as *ADH1*, *PCO1* and *PDC1.* However, the protein level of ERF72 decreased at 24 h after *B. cinerea* infection, suggesting that there exists a fine regulation of ERF protein level for pathogen resistance. (Valeri *et al.*, 2021) One more interesting thing is that, *erfVII* pentuple mutant presents more susceptible to *B. cinerea* infection, however, camalexin content in liquid cultured seedlings of *erfVII* after *B. cinerea* inoculation is similar to that of WT, but that in *erf72* was lower, indicating that different members of ERF-VII play the different role on camalexin biosynthesis and pathogen resistance. The expression of HRE2 was highly induced by *B.cinerea*, which is different from the expression pattern of other ERFVII member (Valeri *et al.*, 2021), indicating HRE2 may have different function in response to *B.cinerea*. Zhao *et al* (2012) showed that overexpression of *RAP2.2* (ERF75) increased resistance to *B. cinerea* in *Arabidopsis,* which further

proved by our results, indicating that ERF72 and RAP2.2 may act redundantly in *B. cinerea* resistance in *Arabidopsis*.

WRKY33 is well proved as a critical defence regulator which is activated by MAPK cascade mediated phosphorylation, and up-regulates the expression of *ORA59*, *ERF1* and *ERF5* in response to *B. cinerea* infection (Birkenbihl *et al.*, 2012; Liu *et al.*, 2015; Zheng *et al.*, 2006). Moreover, previous studies showed that ERF6 is also a substrate of MPK3/MPK6 (Meng *et al.*, 2013; Xu *et al.*, 2016). Phosphorylation of ERF6 by MPK3/MPK6 upon *B.cinerea* infection increases ERF6 protein stability, activates the expression of IGS biosynthesis genes, and confers enhanced resistance to *B. cinerea*. In addition, the constitutively active ERF6 (ERF6-4D) bound to the promoters of *WRKY33* using ChIP experiments (Mine *et al.*, 2018). Here, we demonstrated that phosphorylation of ERF72 by MPK3/MPK6 upon *B.cinerea* infection activates the transcription of *PAD3*, *CYP71A13* and *WRKY33* for camalexin biosynthesis and resistance to *B.cinerea* in *Arabidopsis*. And the transient transactivation assay showed that MPK3/MPK6-mediated phosphorylation enhances the transactivation activity of ERF72, which is same as WRKY33 (Zhou *et al.*, 2020). In addition, *PAD3* and *CYP71A13* were also the target genes of WRKY33 (Mao *et al.*, 2011; Zhou *et al.*, 2020). Taken together, our results suggested that there exists a fine-tuning transcriptional regulation mechanism for the biosynthesis of camalexin in response to *B. cinerea* infection in plants.

Acknowledgements

We thank Dr. Juan Xu (Zhejiang University) for providing the seeds of transgenic *Arabidopsis* line *MPK6SR* and Dr. Michael J. Holdsworth (University of Nottingham) for providing the *erfVII* pentuple mutant. We also acknowledge the Experimental Technology Center for Life Sciences, Beijing Normal University for experimental equipment utilization. This work was supported by the National Natural Science Foundation of China (grant no. 31070250 and 31970723).

Authors' Contributions

Y. L., H. Z., Y. W., D. R. and S. H. designed the project; Y. L., K. L., G. T., C. X. and J. L. performed the experiment and collected the data; Y. L. and S. H. wrote the manuscript. All authors have read the manuscript.

Competing Interests

The authors declare no competing interests.

Data availability

Sequence data from this study can be found in the Arabidopsis Genome Initiative or GenBank/EMBL databases under the following accession numbers: *ERF72* (At3g16770), *WRKY33* (AT2G38470), *CYP71A13* (AT2G30770), *PAD3* (AT3G26830), *PDF1.2* (AT5G44420), *ADH1* (AT1G77120), *PDC1* (AT4G33070), *PCO1* (AT5G15120), *MPK3* (AT3G45640), *MPK6* (AT2G43790), *MKK5* (AT3G21220), *AtActin2* (At3g18780), *AtRHIP1* (AT4G26410), *UBQ10* (AT4G05320), *BcActinA* (Bcin16g02020). All data supporting the findings of this study are available within the paper and within its supplementary data published online.

References:

Allen MD, Yamasaki K, Ohme-Takagi M, Tateno M, Suzuki M. 1998. A novel mode of DNA recognition by a beta-sheet revealed by the solution structure of the GCC-box binding domain in complex with DNA. EMBO Journal **17**, 5484-5496.

Asai T, Tena G, Plotnikova J, Willmann MR, Chiu WL, Gomez-Gomez L, Boller T, Ausubel FM, Sheen J. 2002. MAP kinase signalling cascade in Arabidopsis innate immunity. Nature **415**, 977-983.

Bednarek P. 2012. Chemical warfare or modulators of defence responses - the function of secondary metabolites in plant immunity. Current Opinion in Plant Biology **15**, 407-414.

Bigeard J, Colcombet J, Hirt H. 2015. Signaling Mechanisms in Pattern-Triggered Immunity (PTI). Molecular Plant **8**, 521-539.

Birkenbihl RP, Diezel C, Somssich IE. 2012. Arabidopsis WRKY33 is a key transcriptional regulator of hormonal and metabolic responses toward Botrytis cinerea infection. Plant Physiology **159**, 266-285.

Bottcher C, Westphal L, Schmotz C, Prade E, Scheel D, Glawischnig E. 2009. The multifunctional enzyme CYP71B15 (PHYTOALEXIN DEFICIENT3) converts cysteine-indole-3-acetonitrile to camalexin in the indole-3-acetonitrile metabolic network of Arabidopsis thaliana. The Plant Cell **21**, 1830-1845.

Catinot J, Huang JB, Huang PY, Tseng MY, Chen YL, Gu SY, Lo WS, Wang LC, Chen YR, Zimmerli L. 2015. ETHYLENE RESPONSE FACTOR 96 positively regulates Arabidopsis resistance to necrotrophic pathogens by direct binding to GCC elements of jasmonate - and ethylene-responsive defence genes. Plant Cell & Environment **38**, 2721-2734.

Chen YC, Wong CL, Muzzi F, Vlaardingerbroek I, Kidd BN, Schenk PM. 2014. Root defense analysis against Fusarium oxysporum reveals new regulators to confer resistance. Scientific Reports **4**, 5584.

Clough SJ, Bent AF. 1998. Floral dip: a simplified method for Agrobacterium-mediated transformation of Arabidopsis thaliana. The Plant Journal **16**, 735–743.

Czechowski T, Stitt M, Altmann T, Udvardi MK, Scheible W-Rd. 2005. Genome-Wide Identification and Testing of Superior Reference Genes for Transcript Normalization in Arabidopsis. Plant Physiology **139**, 5-17.

de Marchi R, Sorel M, Mooney B, Fudal I, Goslin K, Kwasniewska K, Ryan PT, Pfalz M, Kroymann J, Pollmann S, Feechan A, Wellmer F, Rivas S, Graciet E. 2016. The N-end rule pathway regulates pathogen responses in plants. Scientific Reports **6**, 26020.

Dean R, Van Kan JA, Pretorius ZA, Hammond-Kosack KE, Di Pietro A, Spanu PD, Rudd JJ, Dickman M, Kahmann R, Ellis J, Foster GD. 2012. The Top 10 fungal pathogens in molecular plant pathology. Molecular Plant Pathology **13**, 414-430.

Fujimoto SY, Ohta M, Usui A, Shinshi H, Ohme-Takagi M. 2000. Arabidopsis ethylene-responsive element binding factors act as transcriptional activators or repressors of GCC box-mediated gene expression. The Plant Cell **12**, 393-404.

Geu-Flores F, Moldrup ME, Bottcher C, Olsen CE, Scheel D, Halkier BA. 2011. Cytosolic gamma-glutamyl peptidases process glutathione conjugates in the biosynthesis of glucosinolates and camalexin in Arabidopsis. The Plant Cell **23**, 2456-2469.

Gibbs DJ, Lee SC, Isa NM, Gramuglia S, Fukao T, Bassel GW, Correia CS, Corbineau F, Theodoulou FL, Bailey-Serres J, Holdsworth MJ. 2011. Homeostatic response to hypoxia is regulated by the N-end rule pathway in plants. Nature **479**, 415-418.

Gibbs DJ, Md Isa N, Movahedi M, Lozano-Juste J, Mendiondo GM, Berckhan S, Marin-de la Rosa N, Vicente Conde J, Sousa Correia C, Pearce SP, Bassel GW, Hamali B, Talloji P, Tome DF, Coego A, Beynon J, Alabadi D, Bachmair A, Leon J, Gray JE, Theodoulou FL, Holdsworth MJ. 2014. Nitric oxide sensing in plants is mediated by proteolytic control of group VII ERF transcription factors. Molecular Cell **53**, 369-379.

Glawischnig E. 2007. Camalexin. Phytochemistry **68**, 401-406.

Glazebrook J. 2005. Contrasting mechanisms of defense against biotrophic and necrotrophic pathogens. Annual Review of Phytopathology **43**, 205-227.

Hao DY, Ohme-Takagi M, Sarai A. 1998. Unique mode of GCC box recognition by the DNA-binding domain of ethylene-responsive element-binding factor (ERF domain) in plant. Journal of Biological Chemistry **273**, 26857-26861.

Huang PY, Catinot J, Zimmerli L. 2016. Ethylene response factors in Arabidopsis immunity. Journal of Experimental Botany **67**, 1231-1241.

Jiang Y, Yu D. 2016. The WRKY57 Transcription Factor Affects the Expression of Jasmonate ZIM-Domain Genes Transcriptionally to Compromise Botrytis cinerea Resistance. Plant Physiology **171**, 2771-2782.

Kim NY, Jang YJ, Park OK. 2018. AP2/ERF family transcription factors ORA59 and RAP2.3 interact in the nucleus and function together in ethylene responses. Frontier in Plant Science **9**, 1675.

Li B, Meng X, Shan L, He P. 2016. Transcriptional regulation of pattern-triggered immunity in plants. Cell Host & Microbe **19**, 641-650.

Li HY, Xiao S, Chye ML. 2008. Ethylene- and pathogen-inducible Arabidopsis acyl-CoA-binding protein 4 interacts with an ethylene-responsive element binding protein. Journal of Experimental Botany **59**, 3997-4006.

Licausi F, Kosmacz M, Weits DA, Giuntoli B, Giorgi FM, Voesenek LA, Perata P, van Dongen JT. 2011. Oxygen sensing in plants is mediated by an N-end rule pathway for protein destabilization. Nature **479**, 419-422.

Licausi F, Ohme-Takagi M, Perata P. 2013a. APETALA2/Ethylene responsive factor (AP2/ERF) transcription factors: mediators of stress responses and developmental programs. New Phytologist **199**, 639-649.

Licausi F, Pucciariello C, Perata P. 2013b. New role for an old rule: N-end rule-mediated degradation of ethylene responsive factor proteins governs low oxygen response in plants. Journal of Integrative Plant Biology **55**, 31-39.

Liu H, Wang Y, Xu J, Su T, Liu G, Ren D. 2008. Ethylene signaling is required for the acceleration of cell death induced by the activation of AtMEK5 in Arabidopsis. Cell Research **18**, 422-432.

Liu K, Li Y, Chen X, Li L, Liu K, Zhao H, Wang Y, Han S. 2018. ERF72 interacts with ARF6 and BZR1 to regulate hypocotyl elongation in Arabidopsis. Journal of Experimental Botany **69**, 3933-3947.

Liu SA, Kracher B, Ziegler J, Birkenbihl RP, Somssich IE. 2015. Negative regulation of ABA signaling by WRKY33 is critical for Arabidopsis immunity towards Botrytis cinerea 2100. Elife **4**, e07295.

Mao G, Meng X, Liu Y, Zheng Z, Chen Z, Zhang S. 2011. Phosphorylation of a WRKY transcription factor by two pathogen-responsive MAPKs drives phytoalexin biosynthesis in Arabidopsis. The Plant Cell **23**, 1639-1653.

Maruyama Y, Yamoto N, Suzuki Y, Chiba Y, Yamazaki K, Sato T, Yamaguchi J. 2013. The Arabidopsis transcriptional repressor ERF9 participates in resistance against necrotrophic fungi. Plant Science **213**, 79-87.

Meng X, Xu J, He Y, Yang KY, Mordorski B, Liu Y, Zhang S. 2013. Phosphorylation of an ERF transcription factor by Arabidopsis MPK3/MPK6 regulates plant defense gene induction and fungal resistance. The Plant Cell **25**, 1126-1142.

Mengiste T. 2012. Plant immunity to necrotrophs. Annual Review of Phytopathology **50**, 267-294.

Mine A, Seyfferth C, Kracher B, Berens ML, Becker D, Tsuda K. 2018. The Defense Phytohormone Signaling Network Enables Rapid, High-Amplitude Transcriptional Reprogramming during Effector-Triggered Immunity. The Plant Cell **30**, 1199-1219.

Moffat CS, Ingle RA, Wathugala DL, Saunders NJ, Knight H, Knight MR. 2012. ERF5 and ERF6 play redundant roles as positive regulators of JA/Et-mediated defense against Botrytis cinerea in Arabidopsis. PLoS One **7**, e35995.

Møldrup ME, Geu-Flores F, Halkier BA. 2013. Assigning gene function in biosynthetic pathways: camalexin and beyond. The Plant Cell **25**, 360-367.

Nafisi M, Goregaoker S, Botanga CJ, Glawischnig E, Olsen CE, Halkier BA, Glazebrook J. 2007. Arabidopsis cytochrome P450 monooxygenase 71A13 catalyzes the conversion of indole-3-acetaldoxime in camalexin synthesis. The Plant Cell **19**, 2039-2052.

Nakano T, Suzuki K, Fujimura T, Shinshi H. 2006. Genome-wide analysis of the ERF gene family in Arabidopsis and rice. Plant Physiology **140**, 411-432.

Oliver RP, Ipcho SV. 2004. Arabidopsis pathology breathes new life into the necrotrophs-vs.-biotrophs classification of fungal pathogens. Molecular Plant Pathology **5**, 347-352.

Piasecka A, Jedrzejczak-Rey N, Bednarek P. 2015. Secondary metabolites in plant innate immunity: conserved function of divergent chemicals. New Phytologist **206**, 948-964.

Pieterse CM, Leon-Reyes A, Van der Ent S, Van Wees SC. 2009. Networking by small-molecule hormones in plant immunity. Nature Chemical Biology **5**, 308-316.

Pre M, Atallah M, Champion A, De Vos M, Pieterse CM, Memelink J. 2008. The AP2/ERF domain transcription factor ORA59 integrates jasmonic acid and ethylene signals in plant defense. Plant Physiology **147**, 1347-1357.

Qiu JL, Fiil BK, Petersen K, Nielsen HB, Botanga CJ, Thorgrimsen S, Palma K, Suarez-Rodriguez MC, Sandbech-Clausen S, Lichota J, Brodersen P, Grasser KD, Mattsson O, Glazebrook J, Mundy J, Petersen M. 2008. Arabidopsis MAP kinase 4 regulates gene expression through transcription factor release in the nucleus. EMBO Journal **27**, 2214-2221.

Ren D, Liu Y, Yang KY, Han L, Mao G, Glazebrook J, Zhang S. 2008. A fungal-responsive MAPK cascade regulates phytoalexin biosynthesis in Arabidopsis. Proceeding in National Academy Science USA **105**, 5638-5643.

Schuhegger R, Nafisi M, Mansourova M, Petersen BL, Olsen CE, Svatos A, Halkier BA, Glawischnig E. 2006. CYP71B15 (PAD3) catalyzes the final step in camalexin biosynthesis. Plant Physiology **141**, 1248-1254.

Sorensson C, Lenman M, Veide-Vilg J, Schopper S, Ljungdahl T, Grotli M, Tamas MJ, Peck SC, Andreasson E. 2012. Determination of primary sequence specificity of Arabidopsis MAPKs MPK3 and MPK6 leads to identification of new substrates. Biochemistry Journal **446**, 271-278.

Su T, Xu J, Li Y, Lei L, Zhao L, Yang H, Feng J, Liu G, Ren D. 2011. Glutathione-indole-3-acetonitrile is required for camalexin biosynthesis in Arabidopsis thaliana. The Plant Cell **23**, 364-380.

Valeri MC, Novi G, Weits DA, Mensuali A, Perata P, Loreti E. 2021. Botrytis cinerea induces local hypoxia in Arabidopsis leaves. New Phytologist **229**, 173-185.

Vicente J, Mendiondo GM, Pauwels J, Pastor V, Izquierdo Y, Naumann C, Movahedi M, Rooney D, Gibbs DJ, Smart K, Bachmair A, Gray JE, Dissmeyer N, Castresana C, Ray

RV, Gevaert K, Holdsworth MJ. 2019. Distinct branches of the N-end rule pathway modulate the plant immune response. New Phytology **221**, 988-1000.

Waadt R, Schmidt LK, Lohse M, Hashimoto K, Bock R, Kudla J. 2008. Multicolor bimolecular fluorescence complementation reveals simultaneous formation of alternative CBL/CIPK complexes in planta. The Plant Journal **56**, 505-516.

Wang M-Y, Liu X-T, Chen Y, Xu X-J, Yu B, Zhang S-Q, Li Q, He Z-H. 2012. Arabidopsis acetyl-amido synthetase GH3.5 involvement in camalexin biosynthesis through conjugation of indole-3-carboxylic acid and cysteine and upregulation of camalexin biosynthesis genes. Journal of Integrative Plant Biology **54**, 471-485.

Weits DA, Giuntoli B, Kosmacz M, Parlanti S, Hubberten HM, Riegler H, Hoefgen R, Perata P, van Dongen JT, Licausi F. 2014. Plant cysteine oxidases control the oxygen-dependent branch of the N-end-rule pathway. Nature Communications **5**, 3425.

White MD, Kamps JJAG, East S, Taylor Kearney LJ, Flashman E. 2018. The plant cysteine oxidases from Arabidopsis thaliana are kinetically tailored to act as oxygen sensors. Journal of Biological Chemistry **293**, 11786-11795.

Xu C. 2020. Pull-down and Co-immunoprecipitation Assays of Interacting Proteins in Plants. Chinese Bulletin of Botany **55**, 62-68.

Xu J, Meng J, Meng X, Zhao Y, Liu J, Sun T, Liu Y, Wang Q, Zhang S. 2016. Pathogen-responsive MPK3 and MPK6 reprogram the biosynthesis of indole glucosinolates and their derivatives in Arabidopsis immunity. The Plant Cell **28**, 1144-1162.

Xu J, Xie J, Yan C, Zou X, Ren D, Zhang S. 2014. A chemical genetic approach demonstrates that MPK3/MPK6 activation and NADPH oxidase-mediated oxidative burst are two independent signaling events in plant immunity. The Plant Journal **77**, 222-234.

Yang L, Zhang Y, Guan R, Li S, Xu X, Zhang S, Xu J. 2020. Co-regulation of indole glucosinolates and camalexin biosynthesis by CPK5/CPK6 and MPK3/MPK6 signaling pathways. Journal of Integrative Plant Biology **62**, 1780-1796.

Zander M, Thurow C, Gatz C. 2014. TGA transcription factors activate the salicylic acid-suppressible branch of the ethylene-induced defense program by regulating ORA59 expression. Plant Physiology **165**, 1671-1683.

Zhao Y, Hull AK, Gupta NR, Goss KA, Alonso J, Ecker JR, Normanly J, Chory J, Celenza JL. 2002. Trp-dependent auxin biosynthesis in Arabidopsis: involvement of cytochrome P450s CYP79B2 and CYP79B3. Genes Development **16**, 3100-3112.

Zhao Y, Wei T, Yin KQ, Chen Z, Gu H, Qu LJ, Qin G. 2012. Arabidopsis RAP2.2 plays an important role in plant resistance to Botrytis cinerea and ethylene responses. New Phytologist **195**, 450-460.

Zheng Z, Qamar SA, Chen Z, Mengiste T. 2006. Arabidopsis WRKY33 transcription factor is required for resistance to necrotrophic fungal pathogens. The Plant Journal **48**, 592-605.

Zhou J, Wang X, He Y, Sang T, Wang P, Dai S, Zhang S, Meng X. 2020. Differential phosphorylation of the transcription factor WRKY33 by the protein kinases CPK5/CPK6 and MPK3/MPK6 cooperatively regulates camalexin biosynthesis in Arabidopsis. The Plant Cell **32**, 2621-2638.

Zong W, Tang N, Yang J, Peng L, Ma S, Xu Y, Li G, Xiong L. 2016. Feedback regulation of ABA signaling and biosynthesis by a bZIP transcription factor targets drought-resistance-related genes. Plant Physiology **171**, 2810-2825.

Figure legend

Fig. 1. ERF72 positively regulates resistance against *B. cinerea* infection and camalexin biosynthesis.

A The typical *B. cinerea* infection phenotype in 4-week-old detached leaves of WT, *erf72*, complementation of wild type form of *ERF72* lines (Com-MC #3 and #9, *pERF72:(MC)ERF72-HA* in *erf72*), and overexpression of *ERF72* lines (ERF72ox #107 and #108, *p35S:(MC)ERF72-HA* in WT) by drop-inoculation with *B. cinerea* spores (5×10^5 spores/mL) after 2 d. Bar = 1 cm. **B**. Measurement of lesion diameters on indicated infected leaves in (A). In box plots, boxes show the interquartile range (IQR) 25–75%, the inner line represents the median, the inner cross represents the mean, and whiskers show the min/max range. The data were collected from 30–40 leaves. Different letters indicate significant differences at $P < 0.05$ determined by One-way ANOVA **C**. Camalexin production was measured from liquid cultured seedling of Com-MC #3 and #9, and ERF72ox #107 and #108 with *B. cinerea* spores (5×10^5 spores/mL) treatment. Bars represent means ± SD, n=3. FW, fresh weight. Different letters indicate significant differences at $P < 0.05$ determined by One-way ANOVA at each time-point. **D**. Protein levels of ERF72 in 14-day-old seedling of complemented and overexpressed lines in response to *B. cinerea* infection at different time points. ERF72 was immunoblotted using an anti-HA antibody; Actin was immunoblotted with its antibody and served as sample loading control.

Fig. 2. ERF72 directly regulates the expression of *PAD3* and *CYP71A13*.

A. The transcriptional levels of camalexin biosynthesis genes *PAD3* and *CYP71A13* (A13) were detected by qRT-PCR in WT and *erf72*. 14-day-old liquid-cultured seedling were inoculated with *B. cinerea* spores at the indicated time points. *RGS1-HXK1 interacting protein 1* (*AtRHIP1,* At4G26410) was used as an internal control. Three biological replicates were examined with similar results, and Data are means ± SD. * and ** indicates significant difference at P <0.05 and P < 0.01 according to Student's *t* test, respectively. **B**. ERF72 activates the transcriptional activity of *PAD3* and *CYP71A13* promoter, respectively. The promoter of *PAD3* or *A13* was fused to GUS (*pPAD3:GUS* or *pA13:GUS*) as a reporter, which was co-transformed with *p35S:(MA)ERF72-HA* or *p35S::GFP* in *Arabidopsis* mesophyll protoplasts. *p35S:LUC* as the internal control. The promoter activities presented as the ratio of GUS to LUC activity. Data are mean values ± SD, n = 3. * indicates a significant difference at P < 0.05 according to Student's *t* test. **C**. ChIP-qPCR analysis of ERF72 binding to the GCC-like box of *pPAD3* or *pCYP71A13* in *vivo*. 14-day-old seedlings of *p35S:(MA)ERF72-HA in erf72* were used for ChIP assays. Anti-HA antibody was used for immunoprecipitation, while mouse normal IgG was used as a negative control. Relative enrichment was calculated as the ratio of the input. Data are mean values ± SD, n = 3. ** indicates a significant difference at P < 0.01 according to Student's *t* test. **D**. EMSA was performed to show that ERF72 binds to the GCC-like box in *pPAD3* and *pCYP71A13*. FAM-labelled DNA fragments containing the GCC-like box were used as probes for the DNA binding assay. Red capitalized

letters indicated the point mutant of the probes. Different amounts of unlabelled probe (cold) were used as competitors.

Fig. 3. *WRKY33* is also a target gene of ERF72.

A. Transcription level of *WRKY33* was monitored by qRT-PCR in response to *B. cinerea* infection in WT and *erf72*. 14-day-old liquid-cultured seedling were inoculated with *B. cinerea* spores at the indicated time points. *AtRHIP1* was used as an internal control. Three biological replicates were examined with similar results, Data are means ± SD, and ** indicates significant difference at P < 0.01 according to Student's *t* test. **B**. ERF72 activates *WRKY33* promoter by binding to the GCC box. Wild-type or GCC-mutated *WRKY33* promoter was fused to GUS as a reporter. *pWRKY33(GCC):GUS* or *pWRKY33(mGCC):GUS* was co-transformed with *p35S:(MA)ERF72-HA or p35S::GFP* into *Arabidopsis* mesophyll protoplasts. *p35S:LUC* as the internal control. The promoter activities presented as the ratio of GUS to LUC activity. Data are means ± SD, n = 3. ns indicates no significant difference and ** indicates a significant difference at P < 0.01 according to Student's *t* test. **C**. EMSA showed ERF72 binding to the GCC box of *WRKY33* promoter. His-ERF72-HA protein was incubated with FAM-labelled DNA fragment containing the GCC box, while unlabelled probe (cold) or mutant probe was used as competitors. Red capitalized letters indicated the point mutant of the probes. **D**. ChIP-qPCR analysis showed ERF72 binding to the GCC box in *WRKY33* promoter. DNA-protein complex was extracted from 14-day-old seedlings of *p35S:(MA)ERF72-HA in erf72.* Anti-HA antibody was used for immunoprecipitation, while

mouse normal IgG was used as a negative control. Data are means ± SD, n = 3. ** indicates a significant difference at P < 0.01 according to Student's *t* test.

Fig. 4. ERF72 regulates resistance to *B. cinerea* and camalexin biosynthesis partial dependent on WRKY33

A. *B. cinerea* infection phenotype in 4-week-old detached leaves of WT, *wrky33*, and *ERF72*-overexpressed in *wrky33* lines (ERF72ox/*wrky33* #7 and #8, *p35S:ERF72-HA* in *wrky33*) by drop-inoculation with *B. cinerea* spores for 2 d. Bar = 1 cm. **B**. Lesion diameters on the indicated infected leaves in (a). **C.** Camalexin contents in WT, *wrky33*, and ERF72ox/*wrky33* #7 and #8 plants were measured from 14-day-old liquid-cultured seeding inoculated with *B. cinerea* spores. **D**. The expression of *PAD3* and *CYP71A13* was detected by qRT-PCR in 14-day-old liquid-cultured seedings of WT, *wrky33*, and ERF72ox/*wrky33* #7 and #8 after inoculated with *B. cinerea* spores. *AtRHIP1* was used as an internal control. Three biological replicates were examined with similar results, Data are means ± SD, and different letters indicate the significant difference at each time-point (P < 0.05, one-way ANOVA). **E**. *B. cinerea* infection phenotype in WT, erf72, *wrky33*, and erf72 wrky33 double mutant. 4-week-old detached leaves were drop-inoculated with *B. cinerea* spores for 2 d. Bar = 1 cm. **F**. Lesion diameters on indicated infected leaves in (E). **G**. Camalexin content in WT, *wrky33*, and ERF72ox/*wrky33* #7 and #8 plants were measured from 14-day-old liquid-cultured seeding inoculated with *B. cinerea* spores. In box plots **(B)** and **(F)**, boxes show the IQR 25–75%, the inner line represents the median, the inner cross represents the mean, and whiskers show the min/max range. The data were collected from 30–40 leaves. different letters indicate

significant differences at P < 0.05 as determined by one-way ANOVA. In **(C)** and **(G)**, data represent means ± SD, n =3. Different letters indicate a significant difference at P < 0.05 according to One-way ANOVA at each time-point. FW: fresh weight.

Fig. 5. MPK3 and MPK6 phosphorylate ERF72 at serine 151.

A. Physical interaction of ERF72 with MPK3 or MPK6 in BiFC assay. ERF72-cYFP was co-transfected with MPK3-nYFP or MPK6-nYFP into *Nicotiana benthamiana* leaves. GUS-nYFP and GUS-cYFP serve as negative controls. Scale bar = 50 μm. **B**. In vitro pull-down assay shows the interactions of ERF72 with MPK3 and MPK6. GST, GST-MPK3, or GST-MPK6 was incubated with His-ERF72-HA and pulled down by glutathione Sepharose resin. His-ERF72-HA was detected with anti-HA antibody, and GST-MPK3 and GST-MPK6 detected by anti-GST antibody. **C**. In vitro phosphorylation of ERF72 by activated MPK3 and MPK6. His-ERF72-HA was incubated with different combinations of MPK3, MPK6 and $MKK5^{DD}$. Proteins were separated in a Phos-tag gel, and ERF72 was detected with anti-HA antibody. A regular immunoblot was done for detecting MAPK activation by anti-pERK antibody and ERF72 by anti-HA antibody as a control. **D**. ERF72 was phosphorylated in $MKK5^{DD}$ after DEX treatment. His-ERF72-HA or His-$ERF72^{S151A}$-HA was mix with protein extraction solution from $MKK5^{DD}$ seeding treated with or without DEX. Proteins were separated by Phos-tag gel, then detected by immunoblot with anti-HA antibody. A regular immunoblot was done for detecting MAPK activation by anti-pERK antibody. **E**. ERF72 phosphorylation was performed with protein extracts from WT seedlings inoculated with or without *B. cinerea* spores. Proteins were

separated by Phos-tag gel, then detected by immunoblot with anti-HA antibody. A regular immunoblot was done for detecting MAPK activation by anti-pERK antibody.

Fig. 6. ERF72 phosphorylation by MPK3/MPK6 is required for ERF72 transactivation activity and camalexin biosynthesis.

A. Transcriptional activity of the *WRKY33* promoter was upregulated by ERF72 and ERF72^{S151D}, but not ERF72^{S151A} mutant form. Reporter vector *pWRKY33:GUS*, and internal control, *p35S:LUC*, were co-transfected with or without different forms of ERF72 into *Arabidopsis* mesophyll protoplasts for 16 h, and the activities of GUS and LUC were measured. The promoter activities are presented as the ratio of GUS to LUC activity. Data are means ± SD, *n* = 3. Different letters indicate significant differences (P < 0.05, one-way ANOVA). **B.** ERF72 upregulation of *WRKY33* transcription was enhanced by MKK5^{DD}. *pWRKY33*:GUS and *p35S:LUC* were co-transformed with *p35S:MKK5^{DD}*, *p35S:(MA)ERF72* or *p35S:(MA)ERF72^{S151A}* into *Arabidopsis* mesophyll protoplasts for 16 h. The promoter activities are presented as the ratio of GUS to LUC activity. Data are means ± SD, *n* = 3. Different letters indicate significant differences (P < 0.05, one-way ANOVA). **C.** ERF72 is required for camalexin production in MKK5^{DD} seedlings with DEX treatment. MKK5^{DD} and MKK5^{DD}/*erf72* seedlings grown in liquid culture were treated with 1 μM DEX for 12 or 24 h, and camalexin content was measured. MAPK activation was analysed by immunoblotting with anti-pERK antibody. FW, fresh weight. Data represent means ± SD, *n* = 3. ** indicates the significant difference between two plants at each time-point (P < 0.01, two-way ANOVA). **D.** DEX induction of MKK5^{DD} had a significantly lower effect on *WRKY33*, *PAD3* and *CYP71A13*

transcription in the *erf72* than that in WT background. Gene expression level was detected by qRT-PCR in $MKK5^{DD}$ and $MKK5^{DD}$ in *erf72* seedlings after treated with 1 μM DEX at indicated time points. *AtRHIP1* was used as an internal control. Three biological replicates were examined with similar results, Data are means ± SD, and ** indicates the significant difference between two plants at each time-point ($P < 0.01$, two-way ANOVA).

Fig. 7. Inhibition of ERF72 phosphorylation decreases resistance to *B. cinerea* and camalexin biosynthesis.

A. *B. cinerea* infection phenotype on 4-week-old detached leaves from WT, *MPK6SR* and *ERF72ox* in *MPK6SR* #4 and #5 (*p35S:ERF72-3HA* in *MPK6SR*) by drop inoculation with *B. cinerea* spores with 10 μM NA-PP1, or an equivalent volume of DMSO pre-treatment for 12 h. Bar = 1 cm. **B.** Lesion diameters of infected leaves indicated in **A**. Data were calculated from 30-40 leaves. Data represent means ± SD. Different letters indicate significant differences at each treatment ($P < 0.05$, one-way ANOVA). **C.** Camalexin production after *B. cinerea* infection was detected in 14-day-old liquid-cultured seedlings of WT, *MPK6SR* and *ERF72ox*/*MPK6SR* #4 and #5 with 2 μM NA-PP1 or an equivalent volume of DMSO pre-treatment for 12 h. Bars represent means ± SD. FW, fresh weight. Different letters indicate significant differences between different plant lines at each time-point ($P < 0.05$, two-way ANOVA).

Figure 1

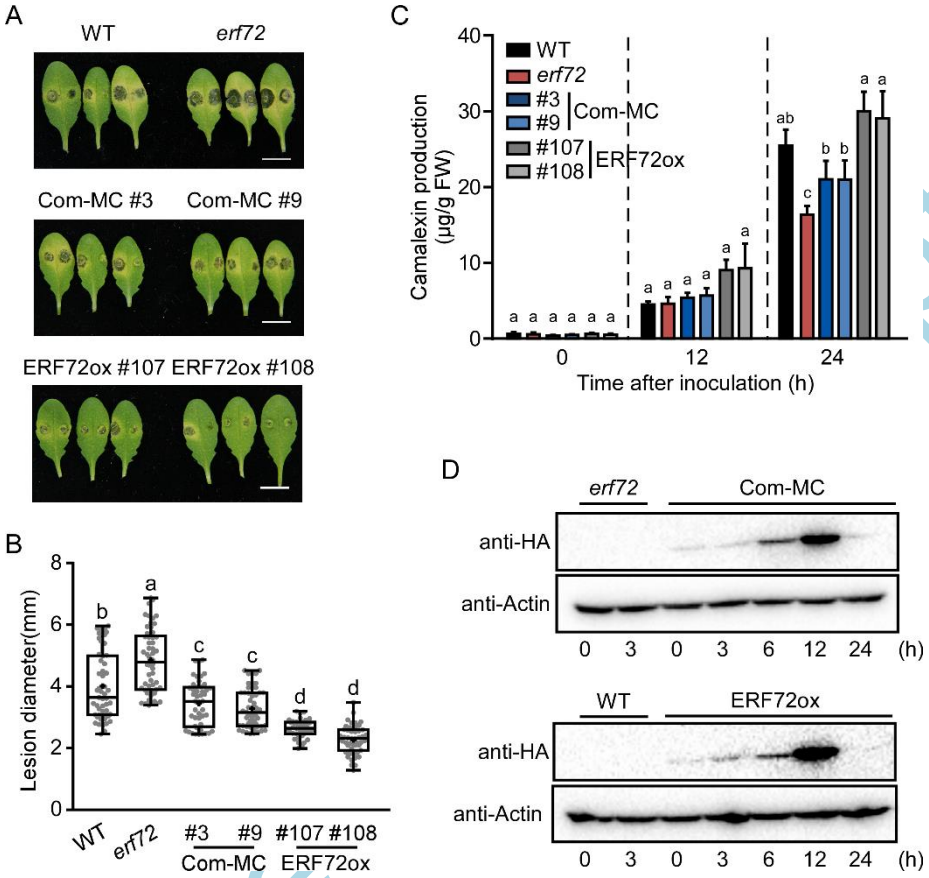

Fig. 1. ERF72 positively regulates resistance against *B. cinerea* infection and camalexin biosynthesis.

A The typical *B. cinerea* infection phenotype in 4-week-old detached leaves of WT, *erf72*, complementation of wild type form of *ERF72* lines (Com-MC #3 and #9, *pERF72:(MC)ERF72-HA* in *erf72*), and overexpression of *ERF72* lines (ERF72ox #107 and #108, *p35S:(MC)ERF72-HA* in WT) by drop-inoculation with *B. cinerea* spores (5×10^5 spores/mL) after 2 d. Bar = 1 cm. **B**. Measurement of lesion diameters on indicated infected leaves in (A). In box plots, boxes show the interquartile range (IQR) 25–75%, the inner line represents the

median, the inner cross represents the mean, and whiskers show the min/max range. The data were collected from 30–40 leaves. Different letters indicate significant differences at $P < 0.05$ determined by One-way ANOVA **C**. Camalexin production was measured from liquid cultured seedling of Com-MC #3 and #9, and ERF72ox #107 and #108 with *B. cinerea* spores (5×10^5 spores/mL) treatment. Bars represent means ± SD, n=3. FW, fresh weight. Different letters indicate significant differences at $P < 0.05$ determined by One-way ANOVA at each time-point. **D**. Protein levels of ERF72 in 14-day-old seedling of complemented and overexpressed lines in response to *B. cinerea* infection at different time points. ERF72 was immunoblotted using an anti-HA antibody; Actin was immunoblotted with its antibody and served as sample loading control.

Figure 2

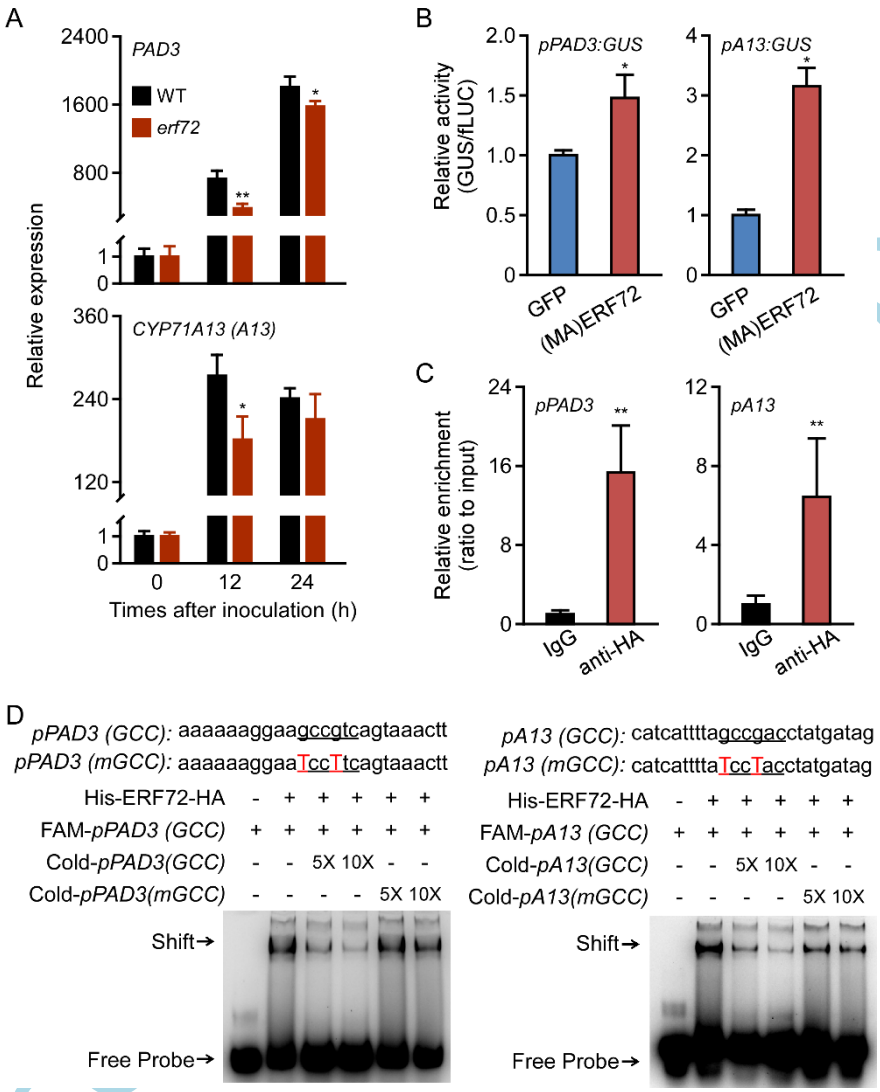

Fig. 2. ERF72 directly regulates the expression of *PAD3* and *CYP71A13*.

A. The transcriptional levels of camalexin biosynthesis genes *PAD3* and *CYP71A13* (A13) were detected by qRT-PCR in WT and *erf72*. 14-day-old liquid-cultured seedling were inoculated with *B. cinerea* spores at the indicated time points. *RGS1-HXK1 interacting protein 1* (*AtRHIP1,* At4G26410) was used as an internal control. Three biological replicates were

examined with similar results, and Data are means ± SD. * and ** indicates significant difference at P <0.05 and P < 0.01 according to Student's *t* test, respectively. **B**. ERF72 activates the transcriptional activity of *PAD3* and *CYP71A13* promoter, respectively. The promoter of *PAD3* or *A13* was fused to GUS (*pPAD3:GUS* or *pA13:GUS*) as a reporter, which was co-transformed with *p35S:(MA)ERF72-HA* or *p35S::GFP* in *Arabidopsis* mesophyll protoplasts. *p35S:LUC* as the internal control. The promoter activities presented as the ratio of GUS to LUC activity. Data are mean values ± SD, n = 3. * indicates a significant difference at P < 0.05 according to Student's *t* test. **C**. ChIP-qPCR analysis of ERF72 binding to the GCC-like box of *pPAD3* or *pCYP71A13* in *vivo*. 14-day-old seedlings of *p35S:(MA)ERF72-HA in erf72* were used for ChIP assays. Anti-HA antibody was used for immunoprecipitation, while mouse normal IgG was used as a negative control. Relative enrichment was calculated as the ratio of the input. Data are mean values ± SD, n = 3. ** indicates a significant difference at P < 0.01 according to Student's *t* test. **D**. EMSA was performed to show that ERF72 binds to the GCC-like box in *pPAD3* and *pCYP71A13*. FAM-labelled DNA fragments containing the GCC-like box were used as probes for the DNA binding assay. Red capitalized letters indicated the point mutant of the probes. Different amounts of unlabelled probe (cold) were used as competitors.

Figure 3

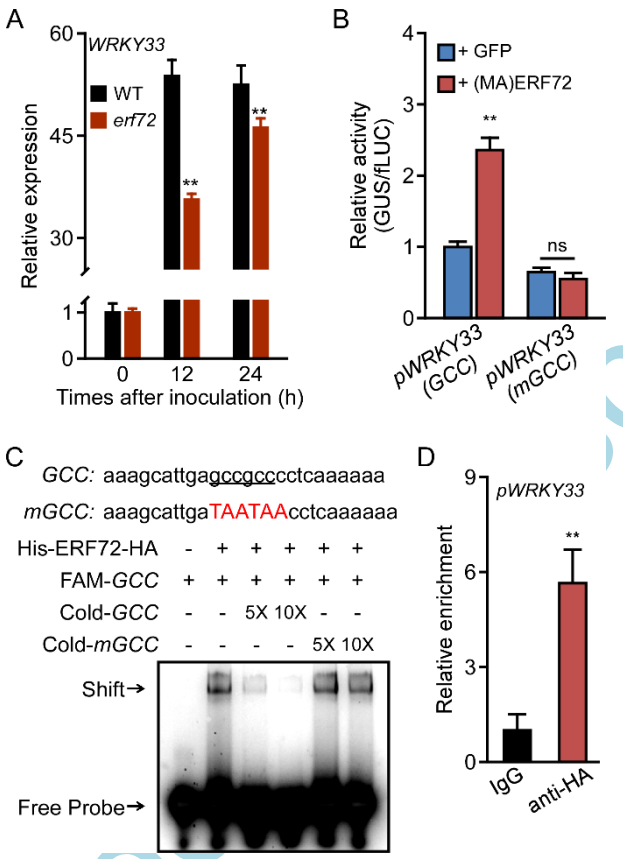

Fig. 3. *WRKY33* is also a target gene of ERF72.

A. Transcription level of *WRKY33* was monitored by qRT-PCR in response to *B. cinerea* infection in WT and *erf72*. 14-day-old liquid-cultured seedling were inoculated with *B. cinerea* spores at the indicated time points. *AtRHIP1* was used as an internal control. Three biological replicates were examined with similar results, Data are means ± SD, and ** indicates significant difference at P < 0.01 according to Student's *t* test. **B**. ERF72 activates *WRKY33* promoter by binding to the GCC box. Wild-type or GCC-mutated *WRKY33* promoter was fused to GUS as a reporter. *pWRKY33(GCC):GUS* or *pWRKY33(mGCC):GUS* was co-

transformed with *p35S:(MA)ERF72-HA or p35S::GFP* into *Arabidopsis* mesophyll protoplasts. *p35S:LUC* as the internal control. The promoter activities presented as the ratio of GUS to LUC activity. Data are means ± SD, n = 3. ns indicates no significant difference and ** indicates a significant difference at P < 0.01 according to Student's *t* test. **C**. EMSA showed ERF72 binding to the GCC box of *WRKY33* promoter. His-ERF72-HA protein was incubated with FAM-labelled DNA fragment containing the GCC box, while unlabelled probe (cold) or mutant probe was used as competitors. Red capitalized letters indicated the point mutant of the probes. **D**. ChIP-qPCR analysis showed ERF72 binding to the GCC box in *WRKY33* promoter. DNA-protein complex was extracted from 14-day-old seedlings of *p35S:(MA)ERF72-HA in erf72.* Anti-HA antibody was used for immunoprecipitation, while mouse normal IgG was used as a negative control. Data are means ± SD, n = 3. ** indicates a significant difference at P < 0.01 according to Student's *t* test.

Figure 4

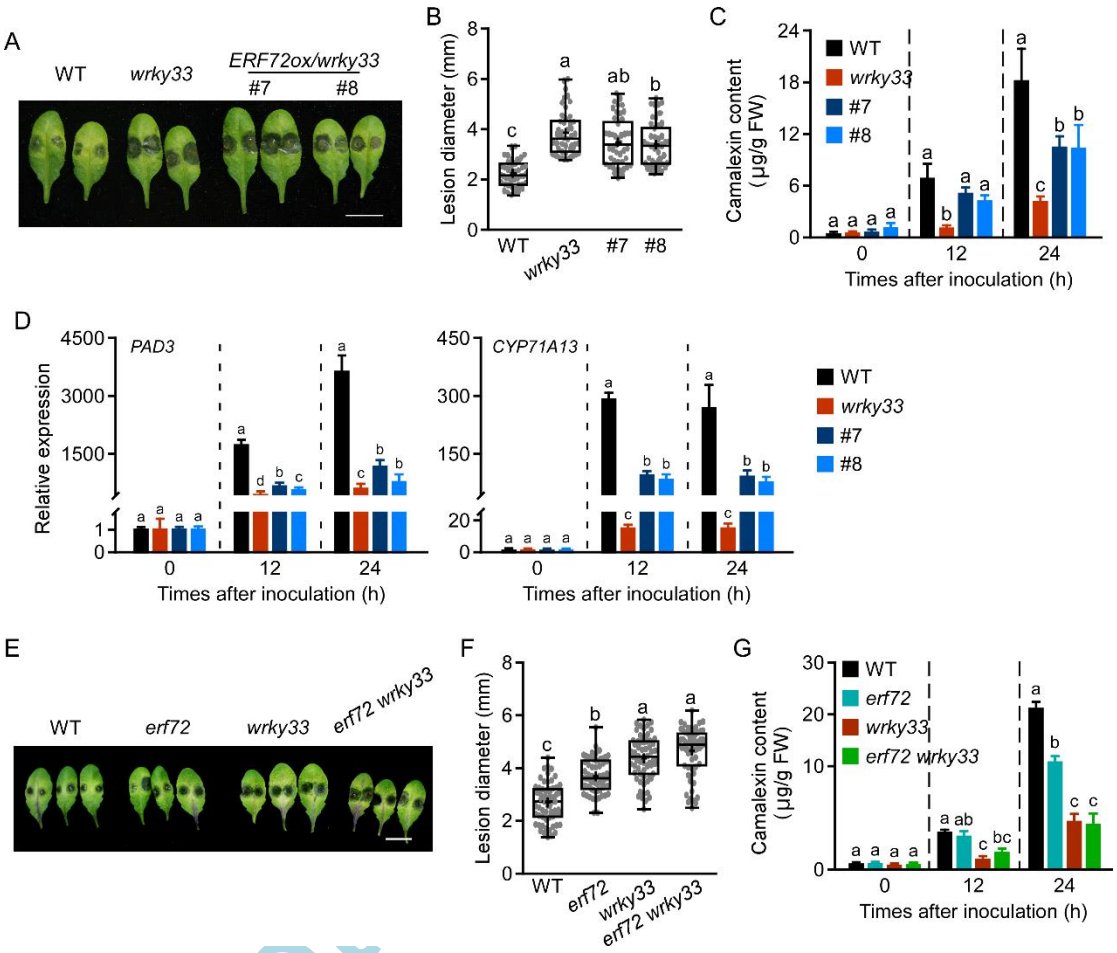

Fig. 4. ERF72 regulates resistance to *B. cinerea* and camalexin biosynthesis partial dependent on WRKY33

A. *B. cinerea* infection phenotype in 4-week-old detached leaves of WT, *wrky33*, and *ERF72*-overexpressed in *wrky33* lines (ERF72ox/*wrky33* #7 and #8, *p35S:ERF72-HA* in *wrky33*) by drop-inoculation with *B. cinerea* spores for 2 d. Bar = 1 cm. **B**. Lesion diameters on the indicated infected leaves in (a). **C.** Camalexin contents in WT, *wrky33*, and ERF72ox/*wrky33* #7 and #8 plants were measured from 14-day-old liquid-cultured seeding inoculated with *B.*

cinerea spores. **D**. The expression of *PAD3* and *CYP71A13* was detected by qRT-PCR in 14-day-old liquid-cultured seedings of WT, *wrky33*, and ERF72ox/*wrky33* #7 and #8 after inoculated with *B*. *cinerea* spores. *AtRHIP1* was used as an internal control. Three biological replicates were examined with similar results, Data are means ± SD, and different letters indicate the significant difference at each time-point ($P < 0.05$, one-way ANOVA). **E**. *B*. *cinerea* infection phenotype in WT, erf72, *wrky33*, and erf72 wrky33 double mutant. 4-week-old detached leaves were drop-inoculated with *B*. *cinerea* spores for 2 d. Bar = 1 cm. **F**. Lesion diameters on indicated infected leaves in (E). **G**. Camalexin content in WT, *wrky33*, and ERF72ox/*wrky33* #7 and #8 plants were measured from 14-day-old liquid-cultured seeding inoculated with *B*. *cinerea* spores. In box plots **(B)** and **(F)**, boxes show the IQR 25–75%, the inner line represents the median, the inner cross represents the mean, and whiskers show the min/max range. The data were collected from 30–40 leaves. different letters indicate significant differences at $P < 0.05$ as determined by one-way ANOVA. In **(C)** and **(G)**, data represent means ± SD, n =3. Different letters indicate a significant difference at $P < 0.05$ according to One-way ANOVA at each time-point. FW: fresh weight.

Figure 5

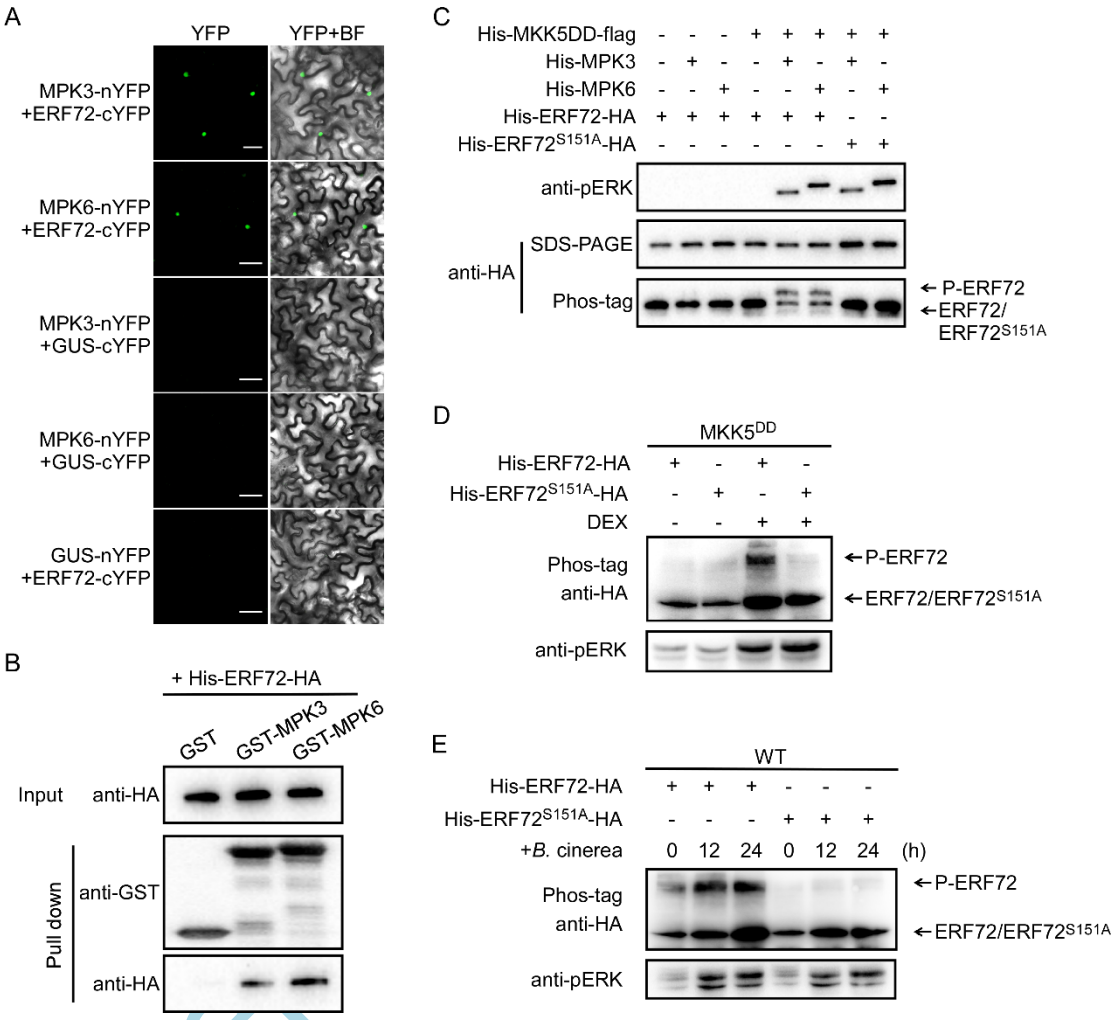

Fig. 5. MPK3 and MPK6 phosphorylate ERF72 at serine 151.

A. Physical interaction of ERF72 with MPK3 or MPK6 in BiFC assay. ERF72-cYFP was co-transfected with MPK3-nYFP or MPK6-nYFP into *Nicotiana benthamiana* leaves. GUS-nYFP and GUS-cYFP serve as negative controls. Scale bar = 50 μm. **B**. In vitro pull-down assay shows the interactions of ERF72 with MPK3 and MPK6. GST, GST-MPK3, or GST-MPK6 was incubated with His-ERF72-HA and pulled down by glutathione Sepharose resin. His-

ERF72-HA was detected with anti-HA antibody, and GST-MPK3 and GST-MPK6 detected by anti-GST antibody. **C**. In vitro phosphorylation of ERF72 by activated MPK3 and MPK6. His-ERF72-HA was incubated with different combinations of MPK3, MPK6 and $MKK5^{DD}$. Proteins were separated in a Phos-tag gel, and ERF72 was detected with anti-HA antibody. A regular immunoblot was done for detecting MAPK activation by anti-pERK antibody and ERF72 by anti-HA antibody as a control. **D**. ERF72 was phosphorylated in $MKK5^{DD}$ after DEX treatment. His-ERF72-HA or His-$ERF72^{S151A}$-HA was mix with protein extraction solution from $MKK5^{DD}$ seeding treated with or without DEX. Proteins were separated by Phos-tag gel, then detected by immunoblot with anti-HA antibody. A regular immunoblot was done for detecting MAPK activation by anti-pERK antibody. **E**. ERF72 phosphorylation was performed with protein extracts from WT seedlings inoculated with or without *B. cinerea* spores. Proteins were separated by Phos-tag gel, then detected by immunoblot with anti-HA antibody. A regular immunoblot was done for detecting MAPK activation by anti-pERK antibody.

Figure 6

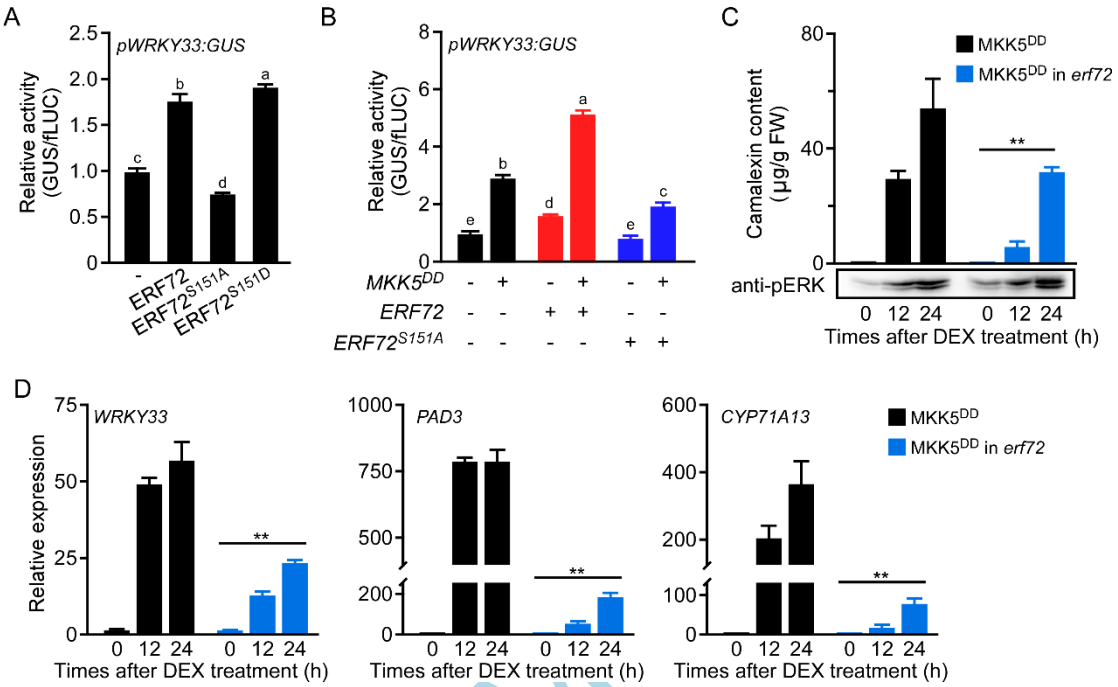

Fig. 6. ERF72 phosphorylation by MPK3/MPK6 is required for ERF72 transactivation activity and camalexin biosynthesis.

A. Transcriptional activity of the *WRKY33* promoter was upregulated by ERF72 and ERF72^{S151D}, but not ERF72^{S151A} mutant form. Reporter vector *pWRKY33:GUS*, and internal control, *p35S:LUC*, were co-transfected with or without different forms of ERF72 into *Arabidopsis* mesophyll protoplasts for 16 h, and the activities of GUS and LUC were measured. The promoter activities are presented as the ratio of GUS to LUC activity. Data are means ± SD, *n* = 3. Different letters indicate significant differences ($P < 0.05$, one-way ANOVA). **B.** ERF72 upregulation of *WRKY33* transcription was enhanced by MKK5^{DD}. *pWRKY33*:GUS and *p35S:LUC* were co-transformed with *p35S:MKK5^{DD}*, *p35S:(MA)ERF72*

or *p35S:(MA)ERF72*^{S151A} into *Arabidopsis* mesophyll protoplasts for 16 h. The promoter activities are presented as the ratio of GUS to LUC activity. Data are means ± SD, *n* = 3. Different letters indicate significant differences (P < 0.05, one-way ANOVA). **C.** ERF72 is required for camalexin production in MKK5^{DD} seedlings with DEX treatment. MKK5^{DD} and MKK5^{DD}/*erf72* seedlings grown in liquid culture were treated with 1 μM DEX for 12 or 24 h, and camalexin content was measured. MAPK activation was analysed by immunoblotting with anti-pERK antibody. FW, fresh weight. Data represent means ± SD, *n* = 3. ** indicates the significant difference between two plants at each time-point (P < 0.01, two-way ANOVA). **D.** DEX induction of MKK5^{DD} had a significantly lower effect on *WRKY33*, *PAD3* and *CYP71A13* transcription in the *erf72* than that in WT background. Gene expression level was detected by qRT-PCR in MKK5^{DD} and MKK5^{DD} in *erf72* seedlings after treated with 1 μM DEX at indicated time points. *AtRHIP1* was used as an internal control. Three biological replicates were examined with similar results, Data are means ± SD, and ** indicates the significant difference between two plants at each time-point (P < 0.01, two-way ANOVA).

Figure 7

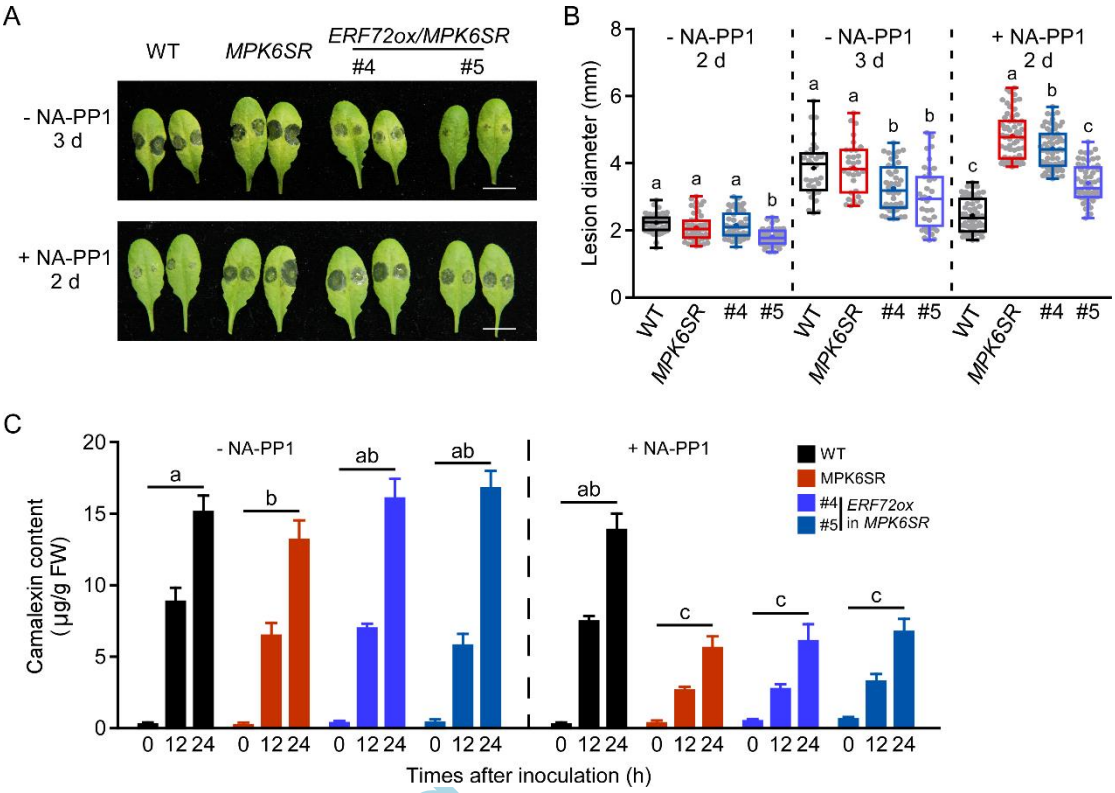

Fig. 7. Inhibition of ERF72 phosphorylation decreases resistance to *B. cinerea* and camalexin biosynthesis.

A. *B. cinerea* infection phenotype on 4-week-old detached leaves from WT, *MPK6SR* and *ERF72ox* in *MPK6SR* #4 and #5 (*p35S:ERF72-3HA* in *MPK6SR*) by drop inoculation with *B. cinerea* spores with 10 μM NA-PP1, or an equivalent volume of DMSO pre-treatment for 12 h. Bar = 1 cm. **B.** Lesion diameters of infected leaves indicated in **A**. Data were calculated from 30-40 leaves. Data represent means ± SD. Different letters indicate significant differences at each treatment ($P < 0.05$, one-way ANOVA). **C.** Camalexin production after *B. cinerea* infection was detected in 14-day-old liquid-cultured seedlings of WT, *MPK6SR* and

ERF72ox/*MPK6SR* #4 and #5 with 2 μM NA-PP1 or an equivalent volume of DMSO pre-treatment for 12 h. Bars represent means ± SD. FW, fresh weight. Different letters indicate significant differences between different plant lines at each time-point ($P < 0.05$, two-way ANOVA).